JPL PUBLICATION 81-48

NASA-CR-164948
19820003225

Nonparametric Identification of a Class of Nonlinear Close-Coupled Dynamic Systems

F. E. Udwadia
Chin-Po Kuo

October 1, 1981

NASA
National Aeronautics and
Space Administration

Jet Propulsion Laboratory
California Institute of Technology
Pasadena, California

JPL PUBLICATION 81-48

Nonparametric Identification of a Class of Nonlinear Close-Coupled Dynamic Systems

F. E. Udwadia
Chin-Po Kuo

October 1, 1981

National Aeronautics and
Space Administration

Jet Propulsion Laboratory
California Institute of Technology
Pasadena, California

The work described in this report was started at the University of Southern California, sponsored by the National Science Foundation, and was completed at the Jet Propulsion Laboratory, California Institute of Technology, under a contract with the National Aeronautics and Space Administration.

The NASA part of the effort was completed in March 1980 in the Applied Mechanics Technology Section at the Jet Propulsion Laboratory, California Institute of Technology, sponsored by Mr. Samuel L. Venneri, Materials and Structures Division, Office of Aeronautics and Space Technology, National Aeronautics and Space Administration.

CONTENTS

CONTENTS (continuation 1)

Figures

CONTENTS (continuation 2)

Figures

ABSTRACT

A nonparametric identification technique for the identification of close coupled dynamic systems with arbitrary memoryless nonlinearities has been presented. The method utilizes noisy recorded data (acceleration, velocity and displacement) to identify the restoring forces in the system. The masses in the system are assumed to be known (or fairly well estimated from the design drawings).

The restoring forces are expanded in a series of orthogonal polynomials and the coefficients of these polynomial expansions are obtained by using least square fit methods. In most mechanical and structural systems, however, the restoring forces can be expressed as a sum of two functions - one related to only the displacement of the system, the other related only to its velocity. The restoring force in this situation is herein referred to as separable. A particularly simple and computationally efficient method has been proposed for dealing with separable restoring forces.

The technique imposes no restrictions on the type of external forcing functions used to test the system. The identified results are found to be relatively insensitive to measurement noise. An analysis of the effects of measurement noise on the quality of the estimates is given.

Several examples have been provided for the identification of close coupled linear and nonlinear dynamic systems. The computations have been shown to be relatively quick (when compared say to the Wiener Identification method) and the core storage required relatively small, making the method perhaps suitable for onboard identification of large space structures.

Nonparametric Identification of a Class of Nonlinear Close-Coupled Dynamic Systems

I. INTRODUCTION

The increased importance given to the accurate prediction of the response of structures in various loading environments, has led, in recent years, to a growing interest in the improvement of methodologies for proper structural modelling. Several investigators have worked in the area of identification of structural systems so as to extract, from various types of response data, improved characterizations of the systems involved [1-6].

The identification problem can be viewed in terms of a class of inputs I, a class of models M and an error criterion, E. It usually takes the following form: Given the system response (at various locations in a structure) to the class of inputs I, identify a member of the class of models M, which minimizes some error criterion E. When sufficient a priori information about the mathematical structure of the class M to which a particular physical system belongs is available, it is often possible to restrict the identification procedure to the determination of the various parameter values, which then characterize the system. Such a procedure is referred to as parametric identification. On the other hand, as often happens for complex structural systems, the a priori information on M may not be sufficient, thus requiring the identification procedure to be "expanded" to a search in function space. This constitutes nonparametric identification and leads to the "best" functional representation of the system. The error criterion E usually takes the form of a norm of the difference between the system performance and the model prediction.

Though a large amount of research has been done in the areas of both parametric and nonparametric identification [7-16], present day techniques for both are, however, deficient when dealing with large structural systems. Parametric methods usually require either the solution of matrix Ricatti equations or the employment of nonlinear programming techniques. Often, when the number of unknowns in the dynamic system exceeds fifty or so these methods in addition to being very computationally expensive may also yield inaccurate estimates. Nonparametric methods which employ the Volterra series or the Weiner Kernel approach are also expensive computationally and often do not provide adequate characterizations of the types of nonlinearities met with in mechanical and structural systems [7-19]. For instance, a "cubic spring" type nonlinearity would require the determination of third order kernels whose computation in practice becomes prohibitively expensive [20]. In addition, the Weiner approach uses white noise inputs. It is often extremely difficult, if not impossible, to generate large enough inputs of this nature so as to drive large (and often massive) dynamic systems in their nonlinear range of response. Applications of such techniques to large, nonlinear, multi-degrees of freedom systems are few, if any.

In this paper we present a relatively simple nonparametric approach for the identification of a class of multi-degrees-of-freedom, close-coupled, nonlinear dynamic systems (Figure 1). The method has the advantage of being computationally efficient and simple to implement on analog or digital machines. Unlike the Weiner Kernel approach, it is not restricted to "white noise" type of inputs, and can be used with almost any type of test input. The choice of the class of models, M, has been governed by its wide usage in problems involving the dynamic response of: (1) full scale building

structures, (2) layered soil masses [21], (3) mechanical equipment [22,23], and (4) machine components and subsystems in, for instance, the nuclear industry [24,25,26].

The technique has been illustrated through application to linear and nonlinear systems, and it has been shown that even under noisy measurement conditions, the method yields good results. An error analysis is also presented to indicate the sensitivity of the method to measurement noise.

II. SYSTEM MODEL

The model consists of a lumped mass system with masses M_ℓ, $\ell = 1,..,N$ which are connected to one another by the unknown memoryless nonlinear elements K_ℓ, $\ell = 1, 2,..,N$ as shown. It is assumed that the acceleration of the base of the structure $\ddot{z}(t)$, and the relative accelerations (with respect to the base) $\ddot{x}_\ell(t)$, $\ell = 1, 2,..,N$ of the various masses are obtained from noisy measurements. The excitation forces $f_\ell(t)$, $\ell = 1,2,...N$ are assumed to be available and the masses M_ℓ, $\ell = 1, 2..,N$, to be either known or fairly well estimated from design drawings.

Further, for the close coupled system shown (Figure 1) it is reasonable to assume that the restoring force K_ℓ depends upon the relative displacement and the relative velocity between the masses M_ℓ and $M_{\ell+1}$. Thus we have

$$K_\ell(t) = K_\ell(y_\ell(t), \dot{y}_\ell(t)), \quad \ell = 1,2,...,N \tag{1}$$

where,

$$y_\ell(t) \triangleq x_\ell(t) - x_{\ell+1}(t), \quad \ell = 1,2,\ldots,N$$

and

$$x_{N+1}(t) \triangleq 0.$$

The dot indicates differentiation with respect to time.

Using noisy measurements of the response $x_\ell(t)$, $\ell = 1,2,\ldots N$, an estimate $\hat{K}_\ell$ of the restoring force K_ℓ is required so that the weighted error norm defined by

$$\varepsilon = \left|\left|\hat{\underline{K}}(y,\dot{y}) - \underline{K}(y,\dot{y})\right|\right|_G \tag{2}$$

is minimized with, G, a suitable weighting matrix and $\underline{K} = \{K_\ell\}$.

The equations of motion governing the system are then given by:

$$\begin{aligned}
&M_1\ddot{x}_1 + K_1[y_1,\dot{y}_1] = - M_1\ddot{z}(t) + f_1(t)\\
&M_2\ddot{x}_2 + K_2[y_2,\dot{y}_2] - K_1[y_1,\dot{y}_1] = - M_2\ddot{z}(t) + f_2(t)\\
&\quad\vdots \qquad\qquad \vdots \qquad\qquad \vdots\\
&M_\ell\ddot{x}_\ell + K_\ell[y_\ell,\dot{y}_\ell] - K_{\ell-1}[y_{\ell-1},\dot{y}_{\ell-1}] = -M_\ell\ddot{z}(t) + f_\ell(t)\\
&\quad\vdots \qquad\qquad \vdots \qquad\qquad \vdots\\
&M_N\ddot{x}_N + K_N[y_N,\dot{y}_N] - K_{N-1}, y_{N-1},\dot{y}_{N-1},y_{N-1}] = - M_N\ddot{z}(t) + f_N(t).
\end{aligned} \tag{3}$$

Equation (3), represents a set of n equations with n unknown restoring forces K_ℓ, $\ell = 1,2,\ldots,N$. The acceleration of each mass and that of the base, as well as the external exciting forces are assumed to be measurable. The objective of the report is to identify the unknown restoring forces from a measured record of time history of the system. We present below two alternative methods for estimating these restoring forces.

Method I:

Adding the top ℓ equations ($\ell = 1,2,\ldots,N$) together at a time, and rearranging, we have the N equations,

$$K_\ell[y_\ell,\dot{y}_\ell] = w_\ell(t), \qquad \ell = 1,2,\ldots,N \tag{4}$$

where

$$w_\ell(t) = \sum_{i=1}^{\ell} \{-M_i[(\ddot{z}(t) + \ddot{x}_i(t)] + f_i(t)\}, \qquad \ell = 1,2,\ldots,N\ . \tag{5}$$

Since $w_\ell(t)$ contains quantities which are either known or available from measurements, the unknown restoring forces $K_\ell(y_\ell,\dot{y}_\ell)$ can be estimated.

Method II:

Equation (3) can be rearranged in the following form:

$$K_\ell[y_\ell,\dot{y}_\ell] = \tilde{\omega}_\ell(t) \qquad \ell = 1,2,\ldots,N \tag{4a}$$

where

$$\tilde{\omega}_{\ell}(t) = -M_{\ell}[\ddot{z}(t) + \ddot{x}(t)] + f_{\ell}(t) + K_{\ell-1}(y_{\ell-1},\dot{y}_{\ell-1})$$

with

$$K_o \triangleq 0$$

In (4a), the restoring force $K_{\ell}(y_{\ell},\dot{y}_{\ell})$ depends on the acceleration of M_{ℓ} and that of the base, the external force, and the restoring force on the previous mass $K_{\ell-1}(y_{\ell-1}, \dot{y}_{\ell-1})$. Noting that $K_o \triangleq 0$, the restoring force on Mass M_1, namely $K_1(y_1,\dot{y}_1)$, can be estimated first; the remaining restoring forces can be obtained by sequentially using equation (4a) for $\ell = 2,\ldots,N$.

III. IDENTIFICATION PROCEDURE

We particularize the identification approach depending on the characteristics of the system under consideration. We consider first, systems with general memoryless restoring forces where the restoring forces K_{ℓ} can be expressed as general analytic functions of y_{ℓ} and $\dot{y}_{\ell}$, and, then, systems with separable restoring forces where the restoring forces K_{ℓ} , $\ell = 1,2,..,N$ can be expressed as a sum of two functions, the first being only dependent on y_{ℓ} and second only on $\dot{y}_{\ell}$.

Whereas the first restoring force situation is more general, the identification procedure in this case requires a larger computing effort. A priori information about the system, especially the foreknowledge that the restoring forces are separable, can be used effectively in reducing the computing effort.

Due to the similarity of the basic concepts between Method I and II described in the previous section, we will devote all our subsequent discussions to Method I unless otherwise stated. The procedure for Method II is similar with slight modifications.

A. General Memoryless Restoring Force:

Assuming that the measurements $\ddot{x}_\ell(t)$, $\ell = 1,2,\ldots,N$ and $\ddot{z}(t)$ are corrupted by Gaussian white noise, we have the measurements

$$\begin{aligned} \hat{\ddot{x}}_\ell(t) &= \ddot{x}_\ell(t) + n_\ell(t), \text{ and} \\ \hat{\ddot{z}}(t) &= \ddot{z}(t) + m(t) \ . \end{aligned} \tag{6}$$

Noisy measurements of the various quanitities are denoted by hats above them. The noise processes may be assumed to have the following characteristics:

$$E[n_i(t_1)\ n_j(t_2)] = \sigma_{\ddot{x}}(t_1)\delta_K(i-j)\delta_D(t_1-t_2),\ i,j = 1,2,\ldots,N$$

$$E[n_i(t)\ m(t_2)] = 0 \qquad i = 1,2,\ldots,N, \text{ and} \tag{7}$$

$$E[m(t_1)m(t_2)] = \delta_{\ddot{z}}(t_1)\delta_D(t_1 - t_2)\ .$$

The symbol E[.] stands for the expected value, δ_D stands for the Dirac-delta function and δ_K for the kroneker delta.

The relative displacements $x_\ell(t)$ and velocities $\dot{x}_\ell(t)$ may be assumed to be either obtained from measurements or from successive integrations of the measured acceleration signals. Thus

$$\hat{x}_\ell(t) = x_\ell(t) + p_\ell(t), \text{ and}$$

$$\hat{\dot{x}}_\ell(t) = \dot{x}_\ell(t) + q_\ell(t), \tag{8}$$

where $p_\ell(t)$ and $q_\ell(t)$, $\ell = 1,2,\ldots,N$, are noise processes. The measurement equation (4) then transforms to

$$\hat{K}_\ell[\hat{y}_\ell\ \hat{\dot{y}}_\ell] = \hat{w}_\ell(t) \triangleq w_\ell(t) + v_\ell(t),\ \ell = 1,2,\ldots,N \tag{9}$$

where

$$v_\ell(t) = \sum_{i=1}^{\ell} - M_i[m(t) + n_i(t)]\ . \tag{10}$$

The function $K_\ell[y_\ell, \dot{y}_\ell]$ can now be expanded in a double series in terms of two sets of functions $\{\phi_n\}$ and $\{\psi_n\}$. Assuming that each set is orthonormal with respect to the weighting functions g_1 and g_2, over suitably defined intervals C_1 and C_2, we have

$$K_\ell[y_\ell, \dot{y}_\ell] \simeq \sum_{j=0}^{J} \sum_{i=0}^{I} a_{ij}^{\ell} \phi_i(y_\ell)\psi_j(\dot{y}_\ell), \quad \ell = 1,2,\ldots,N \tag{11}$$

The coefficients a_{ij}^{ℓ} are to be determined so that the error norm

$$\varepsilon_\ell = ||K_\ell[y_\ell(t), \dot{y}_\ell(t)] - \hat{w}_\ell(t)||_{g_1,g_2}$$

is minimized, say in the least square sense. This yields the estimate

$$\hat{a}_{ij}^{\ell} = \int_{C_2}\int_{C_1} g_1(\hat{y}_\ell)g_2(\hat{\dot{y}}_\ell)\hat{w}_\ell(t)\phi_i(\hat{y}_\ell)\psi_j(\hat{\dot{y}}_\ell)d\hat{y}_\ell d\hat{\dot{y}}_\ell \tag{12}$$

where the measurements $\hat{y}_\ell$ and $\hat{\dot{y}}_\ell$ are used to replace the exact values y_ℓ and $\dot{y}_\ell$.

The response quantities that need to be measured for estimating a specific $K_\ell[y_\ell,\dot{y}_\ell]$, $1 \leq \ell \leq N$ are then $\ddot{x}_i(t)$, $i = 1,2,\ldots,\ell+1$, and $\ddot{z}(t)$.

B. Separable Memoryless Restoring Force:

If it is assumed that

$$K_\ell[y_\ell, \dot{y}_\ell] = R_\ell[y_\ell] + D_\ell[\dot{y}_\ell], \qquad \ell = 1,2...,N \tag{13-A}$$

with

$$R_\ell[0] = D_\ell[0] = 0, \qquad \ell = 1,2,...,N \tag{13-B}$$

then by (4) we have

$$R_\ell[y_\ell] + D_\ell[\dot{y}_\ell] = w_\ell(t), \qquad \ell = 1,2,...,N \tag{14}$$

Again expanding $R_\ell[y_\ell]$ and $D_\ell[\dot{y}_\ell]$ in orthonormal sets $\{\phi_n\}$ and $\{\psi_n\}$ we get

$$R_\ell[y_\ell] \approx \sum_{s=0}^{N_R} b_s^\ell \phi_s(y_\ell), \text{ and}$$

$$D_\ell[\dot{y}_\ell] \approx \sum_{q=0}^{N_D} d_q^\ell \psi_q(\dot{y}_\ell) \ . \tag{15}$$

Estimates of b_s^ℓ and d_q^ℓ can be similarly obtained by minimizing ε_ℓ in the least square sense.

In the case where equation (13) is applicable, a simpler alternative approach may be followed. As $\ddot{x}_\ell(t)$, $\ell = 1,2,\ldots,N$ is measured for $t\varepsilon(0,T)$, the quantities $\hat{y}_\ell(t)$ and $\hat{\dot{y}}_\ell(t)$ can be obtained through integration, if $x_\ell(t)$ and $\dot{x}_\ell(t)$ are not actually measured. Thus times $\hat{t}_{k,\ell}\varepsilon(0,T)$ can be found such that

$$\hat{\dot{y}}_\ell(\hat{t}_{k,\ell}) = 0 \; ; \; k = 1,2,\ldots,k_\ell \quad , \quad \ell = 1,2,\ldots,N \; . \tag{16}$$

For each time $\hat{t}_{k,\ell}$ which satisfies equation (16) the value of $\hat{y}_\ell(t_{k,\ell})$ can be obtained. As the times $\hat{t}_{k,\ell}$ will, because of measurement noise, be slightly different from those at which $\dot{y}_\ell$ equals zero, $D_\ell[\dot{y}_\ell(t_k)]$ though close to zero may not exactly equal it. In fact if $\hat{t}_{k,\ell} = t_{k,\ell} + \tau_{k,\ell}$ where $t_{k,\ell}$ is such that $y_\ell(t_{k,\ell}) = 0$ then using (13),

$$D_\ell[\dot{y}_\ell(\hat{t}_{k,\ell})] = \varepsilon_{D_\ell}(\dot{t}_{k,\ell}) = \left(\frac{dD_\ell}{d\dot{y}_\ell} \cdot \frac{d\dot{y}_\ell}{dt_{k,\ell}} \right) \tau_{k,\ell} \; . \tag{17}$$

Thus

$$R_\ell[y_\ell(\hat{t}_{k,\ell})] = w_\ell(\hat{t}_{k,\ell}) - \varepsilon_{D_\ell}(\hat{t}_{k,\ell}). \tag{18}$$

The coefficients b_s^ℓ, $s = 0,1,2,\ldots N_R$, can now be estimated by minimizing

$$\varepsilon_\ell = \sum_{k=1}^{k_\ell} g_1(y_\ell(t_{k,\ell})) \left[\hat{w}_\ell(\hat{t}_{k,\ell}) - \sum_{s=0}^{N_R} b_s^\ell \phi_s(y_\ell(t_{k,\ell})) \right]^2 \; ; \; \ell = 1,2,\ldots,N \tag{19}$$

Estimates of b_s^{ℓ} then require the solution of the normal equations:

$$\sum_{s=1}^{N_R} \hat{b}_s^{\ell} \, S_{s,j}^{\ell} = T_j^{\ell} \tag{20}$$

where

$$T_j^{\ell} = \sum_{k=1}^{k_\ell} g_1(\hat{y}_\ell(\hat{t}_{k,\ell})) \; \hat{w}_\ell(\hat{t}_{k,\ell}) \; \phi_j(\hat{y}_\ell(\hat{t}_{k,\ell})),$$

$$S_{s,j}^{\ell} = \sum_{k=1}^{k_\ell} g_1(\hat{y}_\ell(t_{k,\ell})) \; \phi_s[\hat{y}_\ell(\hat{t}_{k,\ell})] \; \phi_j[\hat{y}_\ell(t_{k,\ell})] \; , \tag{21}$$

and the quantities $y_\ell(\hat{t}_{k,\ell})$, $k=1,2\ldots,k_\ell$ have been replaced by their estimates $\hat{y}_\ell(t_{k,\ell}) \triangleq \hat{y}_{\ell k}$. By a proper choice of $\{\phi_n\}$ (e.g. Chebyshev polynomials) and by a proper selection of the points $y^*_{\ell k}$ (actually achieved in practice by interpolation), the matrix $S_{s,j}$ may often be made a diagonal matrix, so that

$$\hat{b}_j^{\ell} \approx C_j T_j^{\ell} \tag{22-A}$$

where C_j can be thought of as a normalization constant.

As k_ℓ becomes large, and the measurement noise tends to zero, arbitrarily precise approximations to $R_\ell[y_\ell]$ will be obtained by considering a variety of excitation inputs.

Similarly, the set of points $\hat{t}_{p,\ell} \varepsilon (0,T)$ can be found so that $\hat{y}_\ell(\hat{t}_{p,\ell}) = 0$, $p = 1,2,\ldots,p_\ell$; $\ell = 1,2,\ldots,N$, yielding a normal set of equations similar to (20) and (21), with g_1 replaced by g_2, $\hat{y}_\ell$ replaced by $\hat{\dot{y}}_\ell$ and the functions $\{\phi_n(\hat{y}_\ell)\}$ replaced by $\{\phi_n(\hat{\dot{y}}_\ell)\}$. Again, by a proper choice of $\{\psi_n\}$ and a proper selection of points y^*_{pk}, the estimate of d^ℓ_j can be expressed in the form

$$\hat{d}^\ell_j = E_j \, T^\ell_j \, , \tag{22-B}$$

where E_j is a normalization constant.

The method outlined above, is schematically illustrated (for noise free data) in Figure 2. We begin with the time histories $w_\ell(t)$, $\dot{y}_\ell(t)$ and $y_\ell(t)$, $\ell = 1,2,\ldots,N$. The various times $t_{k,\ell}$, $k = 1,2,..k_\ell$, and $t_{p,\ell}$, $p = 1,2,..p_\ell$, at which $\dot{y}_\ell(t)$ and $y_\ell(t)$ are respectively zero and determined. The values of $y^*_\ell(t_{k,\ell})$ and $\dot{y}^*_\ell(t_{p,\ell})$ corresponding to these times are obtained (Figure 2a). The corresponding restoring forces $R_\ell[y^*(t_{k,\ell})]$ and $D_\ell[\dot{y}^*(t_{p,\ell})]$ are found as $w_\ell[t_{k,\ell}]$ and $w_\ell[t_{p,\ell}]$ respectively. The values of R_ℓ and D_ℓ are then plotted versus y_ℓ and $\dot{y}_\ell$ respectively (Figure 2b).

We mentioned in passing that often sufficient a priori information on the nature of some of the restoring forces may be available, i.e. some of them may be known to be of the separable type. Noting that for purposes of identification, each K_ℓ is uncoupled from the others (equation 4), a combination of the methods presented above can be used - the general case for all the K_ℓ's which have general restoring forces and the separable case for all the K_ℓ's which have separable restoring forces.

C. Forced Vibration Testing of Systems

In the absence of a base motion $\ddot{z}(t)$, the identification of $K_\ell[y_\ell, \dot{y}_\ell]$ can be performed without the need of explicitly knowing (or measuring) the forces $f_i(t)$ if we specify that

$$f_i(t) = \begin{cases} 0 & 1 \leq i \leq \ell, \text{ and} \\ \text{arbitrary} & i > \ell \end{cases} \tag{23}$$

For noise free data, various arbitrary functions $f_i(t)$, $i=\ell$, can be used so that arbitrarily accurate approximations of K_ℓ can be found.

IV. ERROR ANALYSIS

The estimates $\hat{a}^\ell_{ij}$, $\hat{b}^\ell_i$ and $\hat{d}^\ell_i$ obtained by the simple regression analysis technique outlined in the previous sections differ from the exact values primarily because of the presence of measurement noise. The influence of noise may be thought of as affecting: (1) the measured value of $w_\ell(t)$ and (2) the estimates of $y_\ell(t)$ and $\dot{y}_\ell(t)$.

To acquire an appreciation of the effect of measurement noise on the estimates, we shall consider here the case where the restoring force is separable. Error analysis of equation (12) for the general restoring force case, besides being more complex, will not, it appears, yield any additional physical insight into the effect of measurement noise on the estimates.

Let the discrete time points $\hat{t}_{p,\ell}$ be utilized where the times $\hat{t}_{p,\ell}$ are chosen so that, say, $\hat{y}_\ell(\hat{t}_{p,\ell}) = 0$, $p = 1,2\ldots,p_\ell$, $\ell = 1,2\ldots,N$.

If we assume that the noise in measuring, $\ddot{x}(\hat{t}_{p,\ell})$ and $\ddot{Z}_\ell(t_{p,\ell})$, $p = 1,2,\ldots,p_\ell$; $\ell = 1,2,\ldots,N$, has zero mean, is uncorrelated and has a constant variance, then by equation (10),

$$E[v_\ell(\hat{t}_{p,\ell})] = 0, \ \forall\, t \in (0,T), \quad \ell = 1,2,\ldots,N,$$

and

(24)

$$E[v_\ell(\hat{t}_{p,\ell})v_\ell(\hat{t}_{q,\ell})] = \sigma_\ell^2\delta_K(p - q), \ \forall\, \hat{t}_{p,\ell}, \ \hat{t}_{p,\ell}, \ \hat{t}_{q,\ell} \in (0,T) \quad \ell = 1,2,\ldots N,$$

where

$$\sigma_\ell^2 = \sigma_{\ddot{x}}^2(\hat{t}_{p,\ell}) \left(\sum_{i=1}^{\ell} M_i^2\right) + \sigma_{\ddot{z}}^2(\hat{t}_{p,\ell}) \left(\sum_{i=1}^{\ell} M_i\right)^2 \tag{25}$$

Furthermore, if $x_\ell(t)$ and $\dot{x}_\ell(t)$, $\ell = 1,2,\ldots,N+1$ are measured, then we have the following relations:

$$\hat{y}_\ell(\hat{t}_{p,\ell}) = y_\ell(\hat{t}_{p,\ell}) + p_\ell(\hat{t}_{p,\ell}) - p_{\ell+1}(\hat{t}_{p,\ell}) \triangleq y_\ell(\hat{t}_{p,\ell}) + \alpha_\ell(\hat{t}_{p,\ell}) \tag{26-A}$$

and

$$\hat{\dot{y}}_\ell(\hat{t}_{p,\ell}) = \dot{y}_\ell(\hat{t}_{p,\ell}) + q_\ell(\hat{t}_{p,\ell}) - q_{\ell+1}(\hat{t}_{p,\ell}) \triangleq \dot{y}_\ell(\hat{t}_{p,\ell}) + \beta_\ell(\hat{t}_{p,\ell})$$

with $p_{N+1}(t) = q_{N+1}(t) = 0$.

The random variables α_ℓ and β_ℓ are assumed uncorrelated, such that for any two times $t_{p,\ell}$ and $t_{q,\ell} \in (0,T)$,

$$E[\alpha_\ell (\hat{t}_{p,\ell})] = E[\beta_\ell (\hat{t}_{p,\ell})] = 0, \quad \ell = 1,2,\ldots,N,$$

$$E[\alpha_\ell (\hat{t}_{p,\ell})\alpha_\ell (\hat{t}_{q,\ell})] = 2\,\sigma_x^2\,\sigma_K\,(p-q), \quad \ell = 1,2,\ldots,N-1,$$

$$E[\alpha_N (\hat{t}_{p,N})\alpha_N (\hat{t}_{q,N})] = \sigma_x^2\,\delta_k(p-q) \tag{26-B}$$

$$E[\beta_\ell (\hat{t}_{p,\ell})\beta_\ell (\hat{t}_{q,\ell})] = 2\sigma_{\dot{x}}^2\,\delta_K\,(p-q), \quad \ell = 1,2,\ldots,N-1, \text{ and}$$

$$E[\beta_N (\hat{t}_{p,N})\beta_N (\hat{t}_{q,N})] = \sigma_{\dot{x}}^2\,\delta_k(p-q)$$

The variances of the random errors in measuring $x_\ell (\hat{t}_{p,\ell})$ and $\dot{x}_\ell (\hat{t}_{p,\ell})$, $\ell = 1,2,\ldots,N$ are assumed to be σ_x^2 and $\sigma_{\dot{x}}^2$ respectively. The measurements of $z (\hat{t}_{p,\ell})$ and $\dot{z} (\hat{t}_{p,\ell})$ are also corrupted with noise whose variances are σ_z^2 and $\sigma_{\dot{z}}^2$. The various variances could be functions of time.

Let $t_{p,\ell}$ be such that $y_\ell (t_{p,\ell}) = 0$, $P = 1,2,\ldots p_\ell$. (27)

Define $\hat{t}_{p,\ell}$ by the relation

$$\hat{t}_{p,\ell} = t_{p,\ell} + \tau_{p,\ell} \tag{28}$$

where $\tau_{p,\ell}$ is the error in finding $t_{p,\ell}$.

We next expand $y_\ell (\hat{t}_{p,\ell})$ in a Taylor series giving,

$$y_\ell\ (\hat{t}_{p,\ell}) = y_\ell\ (t_{p,\ell}) + \tau_{p,\ell} \frac{dy_\ell}{dt_{p,\ell}} + \frac{\tau^2_{p,\ell}}{2} \frac{d^2 y_\ell}{dt^2_{p,\ell}}$$

$$+ \text{higher order terms} . \tag{29}$$

Using equation (24) and noting relations (26-A) and (23) we get

$$\hat{y}_\ell\ (\hat{t}_{p,\ell}) = 0 \approx \tau_{p,\ell} \frac{dy_\ell}{dt_{p,\ell}} + \alpha_\ell\ (\hat{t}_{p,\ell}) \tag{30}$$

where the higher order terms in $\tau_{p,\ell}$ have been neglected. Thus if

$\dot{y}_\ell\ (t_{p,\ell}) \neq 0$ then

$$\tau_{p,\ell} \approx \alpha_\ell\ (\hat{t}_{p,\ell})\ /\dot{y}_\ell\ (t_{p,\ell}) \triangleq a_{p,\ell}\ \alpha_\ell\ (\hat{t}_{p,\ell}). \tag{31}$$

For the oscillating system considered, it will generally be unlikely that $\dot{y}_\ell(t_{p\ell})$ and $y_\ell(t_{p,\ell})$ be both zero, except when the oscillator is executing very small amplitude motions, preparatory to coming to rest. If, however, $\dot{y}_\ell(t_{p,\ell}) = 0$, then the next higher term in (29) can be used to estimate $\tau_{p,\ell}$.

Then $\hat{w}\ (\hat{t}_{p,\ell})$ can be expanded as

$$\hat{w}_\ell\ (\hat{t}_{p,\ell}) = w_\ell\ (t_{p,\ell}) + a_{p,\ell}\alpha_\ell\ (\hat{t}_{p,\ell}) \frac{dw_\ell}{dt_{p,\ell}} + \frac{a^2_{p,\ell}\alpha^2_\ell\ (\hat{t}_{p,\ell})}{dt^2} \frac{d^2 w_\ell}{dt^2} \tag{32}$$

$$+ \text{higher order terms} + v_\ell(\hat{t}_{p,\ell})$$

and $\hat{\dot{y}}\ (\hat{t}_{p,\ell})$ as

$$\hat{\dot{y}}_\ell\ (\hat{t}_{p,\ell}) = \dot{y}_\ell\ (t_{p,\ell}) + a_{p,\ell}\alpha_\ell\ (\hat{t}_{p,\ell})\ \ddot{y}_\ell\ (t_{p,\ell}) + \frac{a^2_{p,\ell}\ \alpha^2_\ell\ (\hat{t}_{p,\ell})}{2}\ \dddot{y}_\ell(t_{p,\ell})$$

$$+ \text{higher order terms} + \beta_\ell\ (\hat{t}_{p,\ell})\ . \tag{33}$$

Neglecting the higher order terms, equation (33) gives,

$$\hat{\dot{y}}_\ell\ (\hat{t}_{p,\ell}) = \dot{y}_\ell\ (t_{p,\ell}) + \gamma_\ell\ (\hat{t}_{p,\ell}) \tag{34}$$

where,

$$\gamma_\ell\ (\hat{t}_{p,\ell}) = a_{p,\ell}\alpha_\ell\ (\hat{t}_{p,\ell})\ \ddot{y}_\ell\ (t_{p,\ell}) + \frac{a^2_{p,\ell}\alpha^2_\ell\ (t_{p,\ell})}{2}\ \dddot{y}_\ell\ (t_{p,\ell})$$

$$+ \beta_\ell\ (\hat{t}_{p,\ell}), \tag{35}$$

Using equation (22-B), we have

$$\hat{d}_j \approx E_j\ T^\ell_j \approx \sum_{p=1}^{p_\ell} E_j\ \hat{w}_\ell\ (\hat{t}_{p,\ell}) \cdot \tilde{\psi}_j\ (\hat{\dot{y}}_\ell\ (\hat{t}_{p,\ell})) \tag{36}$$

where $\tilde{\psi}_j = g_2\ \psi_j$.

Taking the expected value on both sides of equation (36) we get,

$$E[\hat{d}^\ell_j] \approx \sum_{p=1}^{p_\ell} E_j\ E[\hat{w}_\ell\ (\hat{t}_{p,\ell})\ \tilde{\psi}_j\ (\hat{\dot{y}}_\ell\ (t_{p,\ell}))] \tag{37}$$

The function $\tilde{\psi}_j$ can be expanded about $\dot{y}_\ell(t_{p,\ell})$ to yield, after some manipulation,

$$E[\hat{d}_j^\ell] \approx \sum_{p=1}^{p_\ell} E_j w_\ell(t_{p,\ell})\ \tilde{\psi}_j\ (\dot{y}(t_{p,\ell}))$$

$$+ \sum_{p=1}^{p_\ell} E_j \left\{ E[\alpha_\ell^2(t_{p,\ell})]\ A_{p,\ell} + E[\beta_\ell^2(t_{p,\ell})]\ B_{p,\ell} \right.$$

$$\left. + E[\alpha_\ell^2(t_{p,\ell})]\ E[\beta_\ell^2(t_{p,\ell})]\ G_{p,\ell} \right\} \quad + \text{higher order moment terms} \qquad (38)$$

where

$$A(t_{p,\ell}) = \frac{a_{p,\ell}^2}{2} \left\{ \dddot{y}_\ell w_\ell \frac{d\tilde{\psi}_j}{dy_\ell} + \ddot{y}_\ell^2 w_\ell \frac{d^2\tilde{\psi}_j}{dy_\ell^2} + \ddot{w}_\ell \tilde{\psi}_j + 2\ddot{y}_\ell \dot{w}_\ell \frac{d\tilde{\psi}_j}{d\dot{y}_\ell} \right\}_{t_{p,\ell}}, \qquad (39)$$

$$B(t_{p,\ell}) = \frac{1}{2} \left[w_\ell \frac{d^2\tilde{\psi}_j}{d\dot{y}_\ell^2} \right]_{t_{p,\ell}}, \qquad (40)$$

and,

$$G_{p,\ell} = \frac{1}{4} \left\{ a_{p,\ell}^2\ \ddot{w}_\ell \frac{\partial^2\tilde{\psi}_j}{\partial\dot{y}_\ell^2} \right\}_{t_{p,\ell}}.$$

Similarly it can be shown that

$$E[\hat{b}_j^{\ell}] \approx \sum_{k=1}^{k_\ell} C_j w_\ell(t_{k,\ell})\ \tilde{\phi}_j\ (y_\ell(t_{k,\ell}))$$

$$+ \sum_{k=1}^{k_\ell} C_j \left\{ E[\alpha_\ell^2(t_{k,\ell})]\ A'_{k,\ell} + E[\beta_\ell^2(t_{k,\ell})] B'_{k,\ell} \right.$$

$$\left. + E[\alpha_\ell^2(t_{k,\ell})]\ E[\beta_\ell^2(t_{k,\ell})] G'_{k,\ell} \right\} + \text{higher order moment terms.} \qquad (41)$$

with

$$A'_{k,\ell} = \frac{1}{2}\left[w_\ell \frac{d^2\tilde{\phi}_j}{dy_\ell^2} \right]_{t_{k,\ell}}, \qquad (42)$$

$$B'_{k,\ell} = \frac{b_{k,\ell}^2}{2} \left\{ \ddot{y}_\ell w_\ell \frac{d\tilde{\phi}_j}{dy_\ell} + \dot{y}_\ell^2 w_\ell \frac{d^2\tilde{\phi}_j}{dy_\ell^2} + \ddot{w}_\ell \tilde{\phi}_j + 2\dot{y}_\ell \dot{w}_\ell \frac{d\tilde{\phi}_j}{dy} \right\}_{t_{k,\ell}}, \qquad (43)$$

and,

$$G'_{k,\ell} = \frac{1}{4} \left\{ b_{k,\ell}^2 \ddot{w}_\ell \frac{\partial^2\tilde{\phi}_j}{\partial y^2} \right\}_{t_{k,\ell}},$$

where

$$b_{k,\ell} \triangleq \ddot{y}(t_{k,\ell})^{-1} \quad \text{for} \quad \ddot{y}(t_{k,\ell}) \neq 0, \quad \text{and} \quad \tilde{\phi}_j = g_1\ \phi_j\ .$$

Had the signals x_ℓ and $\dot{x}_\ell$ been obtained by integrating $\ddot{x}_\ell$, the errors α_ℓ and β_ℓ would have been correlated at various times leading to additional terms in equation (40) involving the expected value of the products of $\alpha_\ell\ (t_{p,\ell})$ and $\beta_\ell\ (t_{p,\ell})$.

Equations (38) to (43) indicate the effect of the measurement noise on the expected value of the coefficients b_j^ℓ and d_j^ℓ. We observe that the estimates are biased, the bias being independent of the noise in the measurement of $\ddot{x}_\ell(t)$ and $\ddot{z}_\ell(t)$. The bias is however dependent on the noise in the measurement of $x_\ell(t)$, $\dot{x}_\ell(t)$, $x_{\ell+1}(t)$ and $\dot{x}_{\ell+1}(t)$. If the noise in these measurements goes to zero, (i.e., α_ℓ's and β_ℓ's equal zero) all the terms except the first on the right hand side of equations (38) and (41) go to zero so that the estimates become unbiased. Furthermore, if say, we use the orthonormal polynomials $\{\psi_j\}$ or $\{\phi_j\}$, greater biases would, in general, be obtained for the coefficient estimates $\hat{d}_j^\ell$ and $\hat{b}_j^\ell$ with increasing j. This is because the higher order polynomials oscillate more rapidly thus leading to larger values of the $d\psi_j/d\dot{y}_\ell$, $d^2\psi_j/d\dot{y}_\ell^2$, etc., which in turn, by equations (39) and (41), increase the bias.

Further, to illustrate the effect of noise in the measurement of the acceleration terms, let us assume that $\alpha_\ell(t)$, $\beta_\ell(t)$, $\ell = 1,2,\ldots,N$, are zero. We have then

$$\text{Var}\ [\hat{d}_j^\ell] = E\left[\sum_{p=1}^{p_\ell} v_\ell\ (t_{p,\ell})\ \tilde{\psi}_j\ (\dot{y}_\ell\ (t_{p,\ell}))\right]^2 \tag{44}$$

which for uncorrelated noise gives

$$\text{Var}\,[\hat{d}_j^{\ell}] = \sum_{p=1}^{p_\ell} E[v_\ell^2\,(t_{p,\ell})]\tilde{\psi}_j^2\,(\dot{y}_\ell(t_{p,\ell}))\ . \tag{45}$$

But we have by equation (25)

$$E[v_\ell^2] = \sigma_{\ddot{x}}^2 \sum_{i=1}^{\ell} M_i^2 + \sigma_{\ddot{z}}^2 \left(\sum_{i=1}^{\ell} M_i\right)^2 \tag{46}$$

which indicates that the variance of the estimate increases with ℓ as well as with increasing magnitudes of the masses M_i, $i = 1,2,\ldots,\ell$. Since $M_\ell > 0$, $\forall \ell$, it follows that

$$\left(\sum_{i=1}^{\ell} M_i\right)^2 > \sum_{i=1}^{\ell} M_i^2\ .$$

Thus from equation (43), the variance is more sensitive to noise in the measurement of the base motion $\ddot{z}(t)$, than it is to noise in $\ddot{x}_\ell(t)$, $\ell = 1,2,\ldots,N$.

V. APPLICATIONS

In this section, a few select applications of the identification technique discussed earlier are presented. The responses of the systems considered are simulated by integrating the dynamic equations. Noisy measurement records are obtained by adding zero mean Gaussian white noise (ZMGWN) to the integrated results.

Both the separable and the general restoring force situations have been illustrated. Method I and II (Section II) are applicable to both categories. For the separable restoring force case, the linear system (described below) is identified by Method I using calculations in single precision. On the other hand, the nonlinear systems have been identified by both methods in both single precision and double precision. A comparison of the results of these methods is reported. The general restoring force case is investigated using only computations in single precision.

Motivated by the simplicity of the method, it was attempted to investigate its worthwhileness in a simulated real time environment using a small computer with a maximum core storage of 64KB for computations in single precision. For double precision work, a bigger core was used. A sector of forty seconds of data in each case was analyzed. The digitization rate for the data was taken to be 0.04 sec, a rate which would allow the multiplexing of several channels using standardly available analog-to-digital convectors. The model used is a four degree-of-freedom system as shown in Fig. 3.

A. Separable Restoring Force Case.

Three different systems are considered in this category, a linear system and two nonlinear systems.

a) Linear System

Consider the system shown in figure 3 with the restoring forces given by

$$K_\ell[y,\dot{y}] = R_\ell[y] + D_\ell[\dot{y}], \quad \ell = 1,2,3,4.$$

If the system is linear, then

$$\left.\begin{aligned} R_\ell[y] &= b_1^\ell y \quad , \\ \text{and,} \qquad & \\ D_\ell[y] &= d_1^\ell y \quad . \end{aligned}\right\} \quad \ell = 1,2,3,4. \tag{47}$$

The various parameters of the system are shown in Table 1. The system is subjected to the swept-sine wave test excitation,

$$f_\ell(t) = a_\ell \mathrm{Sin}[\omega(t)]t \qquad i = 1,2,3,4 \tag{48}$$

where the time dependent frequency $\omega(t)$ changes linearly on the time interval, (0,T) according to the relation,

$$\omega(t) = \alpha_1 + \alpha_2 t \tag{49}$$

where,

$$\alpha_2 = \frac{n_1\alpha_1}{n_2 T_0} \quad , \tag{50}$$

n_1 and n_2 are scaling constants, and T_0 is a normalizing time constant. Figure 4 shows a segment of the excitation signal (described in Table 1) at

each of the four mass levels for α = 2 rad/sec, n = 5, n = 40, $\omega_o \triangleq (2\pi/T_o) = \sqrt{b_1^3/m_3} = 10$, and T = 40 secs. The time scale is shown normalized with respect to T_0. A short portion of the system response to this excitation is indicated in Figure 5. Forty seconds of data (approximately 15 times the fundamental period of the system) are used for the identification. By digitizing this data at equispaced time increments Δt = 0.04, the $\ddot{x}_\ell(t)$, digitized time histories $\dot{x}_\ell(t)$ and $x_\ell(t)$ are obtained.

To study the effect of measurement noise on the identification results, these digitized results are corrupted by the addition of zero mean uncorrelated gaussian noise. The same noise-to-signal ratio (N/S) is used for each of the measurements $\ddot{x}_\ell$, $\dot{x}_\ell$, x_ℓ, ℓ = 1,2,3,4. The identification results are obtained for three different values of the N/S ratio, namely, 0.001, 0.01 and 0.02. Whereas the first number represents data of exceptionally good quality, the second typically represents the situation pertinent to data available from accelerographs, and, the third to what may be referred to as "poor" quality data.

From these 'noisy' measurements, the corresponding time histories $\hat{\dot{y}}_\ell(t)$, $\hat{y}_\ell(t)$ and $\hat{w}_\ell(t)$ are calculated for t = iΔt, i=0,1,2,..., 1000.

The functions R_ℓ and D_ℓ are expanded in a series of Chebychev polynomials $\{T_n\}$ so that,

$$R_\ell[y_\ell] \approx \sum_{s=0}^{N_R} \underset{\sim}{b}_s^\ell T_s(y_\ell) = \sum_{s=0}^{N_R} b_s^\ell y_\ell^s \quad ,$$

and (51)

$$D_\ell[\dot{y}_\ell] \approx \sum_{q=0}^{N_D} \underset{\sim}{d}_q^\ell T_q(\dot{y}_\ell) = \sum_{q=0}^{N_D} d_q^\ell \dot{y}_\ell^q$$

The values of N_R and N_D are chosen to be 4 and 3 respectively. The coefficient estimates $\hat{\underset{\sim}{b}}_s^\ell$ and $\hat{\underset{\sim}{d}}_q^\ell$ are obtained (by performing a least square fit) by solving the normal equations (Equations (20) and (21)) [27]. To improve the quality of the fit [27], the $\hat{y}(t_{k,\ell})$ and $\hat{\dot{y}}(t_{p,\ell})$ arrays are normalized so that they lie in the interval (-1,1). Using the weighting functions $g_1(n) = g_2(n) = (1-n^2)^{-1/2}$, the coefficients $\hat{\underset{\sim}{b}}_s^\ell$ and $\hat{\underset{\sim}{d}}_q^\ell$ are found. For ease of comparison with the exact R_ℓ's and D_ℓ's, these coefficients are converted to $\hat{b}_s^\ell$ and $\hat{d}_q^\ell$ corresponding to the polynomial expansions (Equation 51).

Figure 6 shows the results of the identification giving the estimates of the intermass stiffness (R_ℓ) and the intermass damping (D_ℓ) as functions of relative displacement and velocity respectively. The least square polynomial fits are calculated at the various points $\hat{y}(t_{k,\ell})$ and $\hat{\dot{y}}(t_{k,\ell})$ for various noise-to-signal ratios. The exact stiffness and damping are also plotted at the same values of $\hat{y}$ and $\hat{\dot{y}}$ for comparison. As seen from the figure, the

estimates gradually worsen with increasing values of N/S. The estimated coefficients of the polynomials are shown in Table 2(a) and (b) for each R_ℓ and D_ℓ, $\ell = 1,2,3,4$. We observe that, in each case, the estimated coefficients for all except the linear term are small.

A measure of the accuracy of the identified stiffness and damping can be obtained by defining the root mean square errors (rms) as

$$\left.\begin{aligned} \varepsilon_\ell &= \left[\frac{\int [R_\ell - \hat{R}_\ell]^2 dy_\ell}{\int R_\ell^2 dy_\ell}\right]^{1/2}, \quad \text{and} \\ \eta_\ell &= \left[\frac{\int [D_\ell - \hat{D}_\ell]^2 d\dot{y}_\ell}{\int D_\ell^2 d\dot{y}_\ell}\right]^{1/2}, \end{aligned}\right\} \tag{52}$$

where the integrations are carried out over the complete response range of y_ℓ and $\dot{y}_\ell$ respectively. The rms errors are indicated for each R_ℓ and D_ℓ and each N/S ratio in Tables 2(a) and 2(b).

It is interesting to note that the rms error does not change substantially when the N/S ratio changes from 0.001 to 0.01. This is because of the fact that for such low values of the N/S ratio the digitization process as well as the single precision accuracy of the computations (which leads to round off) actually dominates the accuracy of the results. We note from the tables that, in accordance with our discussion in Section IV, the rms error increases with increasing 'i' values.

A comparison of the predicted response using $\hat{R}_\ell$ and $\hat{D}_\ell$ and the exact response for an excitation different from the test excitation, and comprising a base acceleration, $\ddot{z}(t)$, is indicated in Figure 7(a). This base acceleration is actually a sample of zero mean Gaussian White Noise (ZMGWN) with a standard deviation (σ) of unity. The stiffness and damping estimates corresponding to the N/S = 0.02 case are used. We observe that the predicted responses, using the identification results obtained even under very noisy test conditions (N/S = 0.02), and the exact responses are reasonably close to each other.

The solid lines in Figure 7(b) show the response of the system when mass M_1 is subjected to an impulsive (delta-function) force of ten units. The predicted response of the system, using the identification results obtained for N/S = 0.02 (Tables 2a and 2b), is indicated by the dashed lines. Again, the predicted response matches well with the exact response.

b) Nonlinear Systems

Two nonlinear systems have been considered. They represent nonlinearities which are often encountered in structural and mechanical systems. The first system has nonlinear stiffness and linear damping of the form,

$$\left.\begin{aligned} R_\ell[y_\ell] &= b_1^{\ell y}{}_\ell + b_3^{\ell y 3}{}_\ell \\ \text{and} \\ D_\ell[\dot{y}_\ell] &= d_1^{\ell \dot{}} y_\ell \end{aligned}\right\} \quad \ell = 1,2,3,4$$

The system description is given in Table 3. This system is identified by method I using single precision computations. We note that whereas R_1, R_2, R_3

represent 'hardening' nonlinearities, R_4 represents a 'softening' nonlinearity. The test signal used is identical to that used for the linear system described in Table 1. Using $N_R = 4$ and $N_D = 3$, $\hat{\underset{\sim}{b}}_s^{\ell}$ and $\hat{\underset{\sim}{d}}_q^{\ell}$ were obtained. The estimated functions R_ℓ and D_ℓ are shown, as before, in Figure 8. Tables 4a and 4b give the estimates for the coefficients of the polynomial series representation of R_ℓ and D_ℓ. The coefficients are obtained via the Chebychev polynomial expansion as mentioned earlier. The rms values for different N/S ratios are also indicated. It is seen that the identification procedure leads to fairly good estimates even when using noisy (N/S = 1/50) test data.

Figure 9(a) shows a comparison between the predicted response of the system (using the identification results of Tables 4(a) and 4(b)) and the exact response of the system when the system is subjected to twice the amplitude of the ZMGWN base acceleration used before (Figure 7(a)). Identification results corresponding to the N/S ratio of 0.02 were used. Figure 9(b) shows the predicted and actual system response to an impulsive force of ten units applied to mass M_1.

Secondly, a system with nonlinear stiffness and nonlinear damping is chosen and identified by both method I and method II. The system used is the one with

$$\left.\begin{aligned} R_\ell[y_\ell] &= b_1^\ell y_\ell + b_3^\ell y_\ell^3 \quad , \\ \text{and} \qquad & \\ D_\ell[\dot{y}_\ell] &= d_1^{\ell\cdot} \dot{y}_\ell + d_3^{\ell\cdot} \dot{y}_\ell^3 \quad . \end{aligned}\right\} \quad \ell = 1,2,3,4$$

Table 5 shows the actual parameters of the system. Identification of the coefficients $\hat{\underset{\sim s}{b}}^{\ell}$ and $\hat{\underset{\sim q}{d}}^{\ell}$ is done using $N_R = N_D = 3$ in both methods with the test signal defined in Table 1. Since the records of the system are obtained through the integration of the dynamic equation of the system. The accuracy of computation may be one of the factors which affect the estimated functions. An additional double precision calculation, besides a usual single precision calculation, is used in both methods. The estimated functions R_ℓ and D_ℓ done by method I in single precision calculation for different N/S ratios as well as the exact functions are plotted in Figure 10. The response of the actual system and the identified model done by method I and single precision calculation (using results of N/S = .02) subjected to the base acceleration of Figure 7(a) and the same impulsive loading used before are reported in Figure 11(a) and 11(b). Figures (12-14) shows the estimated functions R_ℓ and D_ℓ done by method I and method II in single precision and double precision calculations with various N/S ratios as well as the exact functions. The figures indicate that the accuracy of the functions estimated by both methods is essentially the same. The double precision calculations while requiring more computational effort and core space yield marginal improvements in the estimates. The results of the estimated functions with the RMS errors are shown in Tables 6(a) and 6(b). The RMS errors for method II are seen to be slightly higher than those for method I.

B. The Generalized Restoring Force Case.

Expressing the restoring forces in terms of the orthogonal Chebychev polynominals, we have

$$K_\ell[y_\ell, \dot{y}_\ell] = \sum_{i=1}^{n} \sum_{j=1}^{m} T_i(y_\ell)\ T_j(\dot{y}_\ell)$$

The coefficients a_{ij} are obtained as shown in equation (12) by minimizing the error norm in the least square approach.

Two systems, both nonlinear, have been considered. To compare the general restoring force approach with the separable case, the nonlinear system of Table 3 is identified assuming no a priori knowledge regarding the separability of the restoring force.

A Chebychev polynomial expansion using 64 coefficients (n = m = 8) is employed. The variables $\dot{y}_\ell$ and $\dot{y}_\ell$ are normalized to lie between -1 and +1, and 600 data points are used for the least square fit. The identified coefficients are then converted to monomial bases for ease of comparison with Table 3. Table 7 shows the identification results for different N/S ratios and the RMS errors involved. It is observed that the identified stiffness and damping estimates obtained by this method are in general superior to those obtained using the separable restoring force method. This is attributed not only to the increased number of data points that are used to perform the fit here, but also to the inaccuracies in the separable case that accompany the estimation of the times at which the velocities and displacements become zero.

The second system considered is described by the relation

$$K_\ell[y_\ell,\dot{y}_\ell] = a_\ell y_\ell + b_\ell y_\ell^3 + c_\ell y_\ell \dot{y}_\ell^2 + d_\ell \dot{y}_\ell + e_\ell \dot{y}_\ell^3 + f_\ell \dot{y}_\ell y_\ell^2 \quad ,$$

$$\ell = 1,2,\ldots,N$$

The coefficients a_ℓ, b_ℓ, c_ℓ, d_ℓ, e_ℓ, f_ℓ, $\ell = 1,..,4$, are shown together with the identified results for various N/S ratios in Table 8. The identification is done using 600 data points. The RMS errors are also presented. Perhaps a better way of comparing the identification results with the exact system is to compare $\hat{K}_\ell[y_\ell, \dot{y}_\ell]$ and $K_\ell[y_\ell, \dot{y}_\ell]$. This is done in Figures 15-17 for various N/S ratios. It should be noted that even though some of the identified coefficients differ substantially from those of the actual system, in the regime of response considered, the RMS errors are small. It is these RMS errors which should be, in reality, considered when assessing the quality of the identified results.

VI. CONCLUSIONS AND DISCUSSION

A relatively simple nonparametric method for the identification of a class of close-coupled nonlinear multi-degree-of-freedom systems has been developed. The class of systems is one which is often encountered in the fields of mechanical and structural engineering. Identification of arbitrary memoryless nonlinearities is possible through knowledge of the accelerations, velocities and displacements of the various masses. These quantities are then used to obtain by regression techniques the surfaces of the restoring forces as functions of the intermass displacements and velocities.

A particularly simple and computationally efficient technique is illustrated when the restoring force is linearly separable into two functions, one of intermass velocity and the other of intermass displacement.

An assessment has been made of the effect of measurement noise on the estimates of the coefficients that are obtained from the regression analysis. It is found that whereas the biases in the estimated coefficients are primarily dependent on the noise in the displacement and velocity measurements, their variances are controlled to a good extent by noise in the acceleration measurements.

All the computations related to single precision calculations have been performed on a small 16 bit minicomputer, with a 64KB memory. Even under very noise measurement conditions, (N/S ratio of 1/50) with only a few terms in the series expansion, the identification results yield low rms errors. The capability of predicting the response of the system to excitations other than the test excitation, by using the results from identification, has been illustrated. As has been observed in other studies [7] accurate estimates of the damping are in general more difficult to obtain than estimates of the stiffness. Double precision computations while significantly increasing the computational effort and the core required (beyond 64KB) did not yield substantial improvements in the estimates.

A drawback of the method is that it can only be used for identifying memoryless intermass nonlinear restoring forces. This is so because expansions of the type given by equations (11) and (15), where the y_ℓ's and

$\dot{y}_\ell$'s are treated as independent variables, are only valid if the restoring forces are single valued functions of the independent variables. Thus, for example, in a bilinear hysteretic system in which the restoring force is a multivalued function of y_ℓ and $\dot{y}_\ell$, the technique would fail. Alternatively speaking, for such systems, one could find a class of inputs which would yield incorrect identification. A simple example of such a class of inputs, for the bilinear hysteretic case, is the class of inpulsive excitations which cause permanent displacements of the system.

The main advantages of the method are:

(1) The method is applicable to general memoryless intermass nonlinear restoring forces.

(2) There is no limitation on the nature of the test excitation that can be used for the identification. This is a major advantage over some of the other non-parametric methods [20, 21] which often require Gaussian White Noise (GWN) excitations. Such GWN excitations are difficult to produce in high enough magnitudes in order to drive multi-degree-of-freedom systems, which are often large, in their nonlinear ranges of response.

(3) The computational requirements, both in terms of CPU time as well as storage, are very small in comparison with the Weiner Method making the method attractive for real time identification [21].

(4) The duration of time over which the data is required to be taken is comparatively small compared to other nonparametric techniques [21].

(5) The identification results obtained are relatively insensitive to measurement noise. The rms errors in the determination of the restoring forces increase in general as we move towards the point of fixity of the system.

VII REFERENCES

1. Eykhoff, P. "Process Parameter and State Estimation", Survey Paper, Proc. I.F.A.C. 3rd Congress, London 1966.

2. Berman, A., "System Identification of a Complex Structure", AIAA 16th Structures, Structural Dynamics and Materials Conference, Denver, Colorado.

3. Dale, D.B. and Cohen, R., "Multiparameter Identification in Linear Continuous Vibratory Systems", ASME Journal of Dynamic Systems, Measurements and Control, Vol 93, March 1971.

4. Eshleman, R.A., "System Modeling", The Shock and Vibration Digest, Vol. 4, May 1972, p. 1.

5. Hart, G.C., ed., Dynamic Response of Structures: Instrumentation, Testing Methods and System Identification, ASCE/EMD Specialty Conference, UCLA, 1976.

6. Collins, J.D., et al., Statistical Identification of Structures", AIAA Journal, Vol. 12, 1970, pp. 185-190.

7. Udwadia, F.E. and Jerath, N., "Time Variations of Structural Properties During Strong Ground Shaking", ASCE, EM1, Vol. 106, 1980, pp. 111-121.

8. Beliveau, J.G., "Identification of Viscious Damping in Structures from Model Information", ASME, Journal of Applied Mechanics, Vol. 43, June 1976, pp. 335-339.

9. Distefano, N., and Todeschini, R., "Modeling, Identification and Prediction of a Class of Nonlinear Viscoelastic Materials", International Journal of Solids and Structures Part I, Vol. 9, 1976, pp. 805-818.

10. Udwadia, F.E. and Shah, P.C., "Identification of Structures Through Records Obtained During Strong Earthquake Ground Motion", ASME, Journal of Engineering for Industry, Vol. 98, No. 4, 1976, pp. 1347-1362.

11. Udwadia, F.E. Sharma, D.K. and Shah, P.C., "Uniqueness of Damping and Stiffness Distribution in the Identification of Soil and Structural Systems", ASME Journal of Applied Mechanics, Vol. 45, March 1978, pp. 181-187.

12. Kaya, I. and McNiven, H., "Investigvation of the Elastic Characteristics of a Three Story Steel Frame Using System Identification", Report No. EERC 78/24, Earth Engineering Research Center, University of California, Berkeley, 1978.

13. Hays C., "Inelastic Materials Models in Earthquake Response", Proc. 3rd Engineering Mechanics Specialty Conference, September 17-19, 1979.

14. Beck, J.L., "Determining Models of Structures From Earthquake Records", EERRL 78-01, Caltech, Pasadena, 1978.

15. Ray D., et al, "Sensitivity Analysis of Hysteritic Dynamic Systems: Theory and Application", Comp. Methods in Appl. Mech. and Eng., Vol. 14, 1978, pp. 179-208.

16. Masri, S.F., and Caughey, T.K., "A Nonparametric Identification Technique for Nonlinear Dynamic Problems", ASME, Journal of Applied Mechanics, Vol. 46, June 1979, pp. 433-447.

17. Hudson, D.E., "Dynamic Tests of Full Scale Structures", Earthquake Engineering, Prentice Hall, pp. 127-149.

18. Lee, Y.W., and Schetzen, J., "Measurement of the Weiner Kernels of a Nonlinear System by Cross Correlation", International Journal of Control, Vol. 2, 1965, pp. 237-254.

19. Wiener, N., "Nonlinear Problems in Random Theory", M.I.T. Press, Cambridge, Mass., 1958.

20. Udwadia, F.E. and Marmarelis, P.Z., "The Identification of Building Systems. II The Nonlinear Case", Bull. of the Seismological Soc. of America, Vol. 66, No. 1, February, 1976, pp. 125-151.

21. Udwadia, F.E. and Marmarelis, P.Z., "The Identification of Building Systems. II The Nonlinear Case", Bull. of the Seismological Soc. of America, Vol. 66, No. 1, February, 1976, pp. 153-171.

22. Seed, H.B. and Idriss, I.M., "Analysis of Soil LiquiFaction: Niigata Earthquake", ASCE, SM3, May 1967, p. 83-108.

23. Buzdugan, G.H., and Rades, M., "Forty-fourth Euromechanics Collequium on Dynamics of Machine Foundations", Bucharest, 29-31 Oct., 1973.

24. Hadjian, A.H., "Support Motions for Mechanical Components During Earthquakes", Proceedings of the I. Mech. E. Conference, Nov. 7-9, 1978, pp. 27-46.

25. Hitchings, D., and Beresford, P.J., "A Comparison of Numerical Methods for Seismic Design of Mechanical Systems", I. Mech. E. Proceedings, November 7-9, 1978, pp. 129-138.

26. Kajimura, Y., and Shiraki, K., "Statistical Method of Estimating the Seismic Response of Light Secondary Systems", I. Mech. E. Proceedings, November 7-9, 1978, pp. 207-214.

27. Hamming R., Numerical Methods for Scientists and Engineers, McGraw Hill.

TABLES AND FIGURES

Table 1. Description of linear system

SYSTEM 1 (Stiffness = linear) (Damping = linear)				TEST SIGNAL $f_i(t) = a_i \, Sin[\alpha_1+\alpha_2 t]t$				
i	m_i/m^*	$K_i[y,\dot{y}] = b_1^i y + d_1^i \dot{y}$						
		b_1^i/b^*	d_1^i/d^*	a_i	α_1	n_1	n_2	ω_0
1	1.0	0.50	1.00	10.0	2.0	5	40	10.0
2	1.0	0.75	0.80	-20.0	2.0	5	40	10.0
3	1.0	1.00	0.60	15.0	2.0	5	40	10.0
4	2.0	0.50	2.00	-25.0	2.0	5	40	10.0
m^*=1, b^*=100, d^*=0.5				$T_0 = 2\pi/\omega_0$; $\alpha_2 = (n_1\alpha_1)/(n_2 T_0)$				

Table 2a. The coefficients of the identified stiffness of System 1

i	$R_i = b_1^i y$	N/S	$\hat{R}_i = \hat{b}_0^i + \hat{b}_1^i y + \hat{b}_2^i y^2 + \hat{b}_3^i y^3 + \hat{b}_4^i y^4$					ε_i
	b_1^i		$\hat{b}_0^i$	$\hat{b}_1^i$	$\hat{b}_2^i$	$\hat{b}_3^i$	$\hat{b}_4^i$	
1	50	0.001	-0.00197	48.130	0.59691	2.7956	-1.0551	0.01552
		0.010	-0.00513	48.220	0.35053	2.5490	-0.57827	0.01527
		0.020	-0.01111	48.208	0.15696	2.4581	-0.19538	0.01617
2	75	0.001	-0.01824	74.250	0.23820	0.39391	-0.13063	0.00409
		0.010	0.06529	74.325	-0.07721	0.36444	0.06970	0.00442
		0.020	0.17733	74.335	-0.44445	0.36817	0.27012	0.00607
3	100	0.001	-0.00021	99.436	0.09831	0.47977	-0.10275	0.00232
		0.010	0.06144	99.631	0.01514	0.14904	0.11477	0.00291
		0.020	0.09254	99.732	0.03808	-0.10082	0.25814	0.00452
4	50	0.001	-0.06270	48.997	0.26450	0.62990	-0.01724	0.00906
		0.010	-0.04072	49.149	0.48949	0.51912	-0.30196	0.00896
		0.020	-0.01943	49.240	0.68484	0.44278	-0.56636	0.01198

Table 2b. The coefficients of the identified damping of System 1

i	$D_i = d_1^i \dot{y}$	N/S	$\hat{D}_i = \hat{d}_0^i + \hat{d}_1^i \dot{y} + \hat{d}_2^i \dot{y}^2 + \hat{d}_3^i \dot{y}^3$				η_i
	d_1^i		$\hat{d}_0^i$	$\hat{d}_1^i$	$\hat{d}_2^i$	$\hat{d}_3^i$	
1	0.5	0.001	0.00033	0.51512	-0.00034	0.00008	0.04534
		0.010	-0.07826	0.53241	0.00085	-0.00006	0.05553
		0.020	-0.07995	0.54058	0.00111	-0.00012	0.06109
2	0.4	0.001	0.03075	0.41320	0.00008	0.00000	0.03410
		0.010	-0.06653	0.43327	0.00008	-0.00002	0.06786
		0.020	-0.09249	0.45110	0.00005	-0.00003	0.10025
3	0.3	0.001	-0.00911	0.30483	-0.00001	0.00001	0.02608
		0.010	-0.00942	0.28528	0.00057	0.00009	0.03947
		0.020	0.02597	0.26441	0.00102	0.00016	0.07600
4	1.0	0.001	-0.15991	0.95647	0.00594	0.00218	0.03891
		0.010	-0.35716	0.97538	0.00655	0.00146	0.07359
		0.020	-0.50936	0.98855	0.00550	0.00083	0.11056

Table 3. Description of the system with nonlinear stiffness and linear damping

SYSTEM 2 (Stiffness = nonlinear) (Damping = linear)				
i	m_i/m^*	$K_i[y,\dot{y}] = b_1^i y + b_3^i y^3 + d_1^i \dot{y}$		
		b_1^i/b^*	b_3^i/b^*	d_1^i/d^*
1	1.0	0.50	0.10	1.00
2	1.0	0.75	0.25	0.80
3	1.0	1.00	0.20	0.60
4	2.0	0.50	-0.10	2.00
$m^*=1$, $b^*=100$, $d^*=0.5$				

Table 4a. The coefficients of the identified stiffness of System 2

i	$R_i=b_1^i y+b_3^i y^3$		N/S	$\hat{R}_i = \hat{b}_0^i + \hat{b}_1^i y + \hat{b}_2^i y^2 + \hat{b}_3^i y^3 + \hat{b}_4^i y^4$					ε_i
	b_1^i	b_3^i		$\hat{b}_0^i$	$\hat{b}_1^i$	$\hat{b}_2^i$	$\hat{b}_3^i$	$\hat{b}_4^i$	
1	50	10	0.001	0.00902	48.915	0.22394	11.888	-0.42176	0.00865
			0.010	0.02193	49.039	-0.27482	11.527	0.31841	0.00809
			0.020	0.03476	49.146	-0.76921	11.145	1.0329	0.00815
2	75	25	0.001	-0.02578	74.441	0.02301	25.556	-0.01337	0.00332
			0.010	0.06611	74.486	-0.18270	25.566	0.03328	0.00365
			0.020	0.18139	74.490	-0.45454	25.596	0.10826	0.00425
3	100	20	0.001	-0.00499	99.677	-0.02814	20.525	0.04931	0.00147
			0.010	0.10660	100.160	1.0550	19.993	-1.4486	0.00350
			0.020	0.17982	100.56	2.2282	19.527	-3.0004	0.00701
4	50	-10	0.001	-0.02028	49.627	0.02107	-9.7352	0.08131	0.00458
			0.010	-0.02244	49.146	0.28733	-9.4405	-0.30165	0.01273
			0.020	-0.05730	48.607	0.60696	-9.1306	-0.71023	0.02433

Table 4b. The coefficients of the identified damping of System 2

i	$D_i = b_1^i \dot{y}$	N/S	$\hat{D}_i = \hat{d}_0^i + \hat{d}_1^i \dot{y} + \hat{d}_2^i \dot{y}^2 + \hat{d}_3^i \dot{y}^3$				η_i
	d_1^i		$\hat{d}_0^i$	$\hat{d}_1^i$	$\hat{d}_2^i$	$\hat{d}_3^i$	
1	0.5	0.001	-0.01487	0.52479	-0.00008	0.00005	0.061573
		0.010	0.00218	0.52264	0.00041	0.00003	0.05254
		0.020	-0.00323	0.52365	0.00115	-0.00002	0.04916
2	0.4	0.001	-0.01897	0.40985	-0.00056	0.000004	0.04179
		0.010	-0.01952	0.42118	-0.00070	-0.00001	0.05485
		0.020	0.01377	0.42822	-0.00091	-0.00002	0.06562
3	0.3	0.001	0.00748	0.30273	0.00001	0.00003	0.03412
		0.010	-0.02072	0.30118	0.00049	0.00004	0.03714
		0.020	0.08008	0.29381	0.00043	0.00006	0.05204
4	1.0	0.001	0.08478	1.18900	-0.01297	-0.00428	0.07780
		0.010	-0.30175	1.09520	-0.00124	-0.00217	0.07152
		0.020	-0.64619	1.00790	0.00849	-0.00028	0.10322

Table 5. Description of the system with both nonlinear stiffness and damping

SYSTEM 3 (Stiffness = nonlinear) (Damping = nonlinear)					
i	m_i/m^*	$K_i[y,\dot{y}] = b_1^i y + b_3^i y^3 + d_1^i \dot{y} + d_3^i \dot{y}^3$			
		b_1^i/b^*	b_3^i/b^*	d_1^i/d^*	d_3^i/d^*
1	1.0	0.50	0.10	0.60	0.04
2	1.0	0.75	0.20	0.40	0.04
3	1.0	1.00	0.25	0.40	0.04
4	2.0	0.50	-0.10	0.20	0.04
$m^*=1$, $b^*=100$, $d^*=0.5$					

Table 6a. The coefficients of the identified stiffness of the second nonlinear system done by Method I and Method II in single precision and double precision calculation*.

i	$R_1=b_1^i y+b_3^i y^3$		N/S	Method	Precision	$\hat{R}_i = \hat{b}_0^i + \hat{b}_1^i y + \hat{b}_2^i y + \hat{b}_3^i y^3$				E_i
	b_1^i	b_3^i				$\hat{b}_0^i$	$\hat{b}_1^i$	$\hat{b}_2^i$	$\hat{b}_3^i$	
1	50	10	.001	I	S	-.01686	48.375	-.04161	12.375	.01429
				I	D	-.01670	48.379	-.04171	12.370	.01426
				II	S	-.01686	48.375	-.04161	12.375	.01429
				II	D	-.01670	48.379	-.04171	12.370	.01426
			.01	I	S	-.04644	48.628	-.02344	11.606	.01222
				I	D	-.04626	48.631	-.02362	11.601	.01219
				II	S	-.04644	48.628	-.02344	11.606	.01222
				II	D	-.04626	48.631	-.02362	11.601	.01219
			.02	I	S	-.07220	48.700	-.03593	11.109	.01391
				I	D	-.07202	48.703	-.03615	11.105	.01388
				II	S	-.07220	48.700	-.03593	11.109	.01391
				II	D	-.07202	48.703	-.03615	11.105	.01388
2	75	20	.001	I	S	-.03992	73.254	.10587	22.916	.00962
				I	D	-.04018	73.259	.10634	22.911	.00960
				II	S	-.10122	71.991	.22105	25.168	.01713
				II	D	-.10089	71.997	.22135	25.159	.01710
			.01	I	S	.05966	73.669	-.06598	22.185	.00734
				I	D	.05936	73.674	-.06540	22.180	.00732
				II	S	-.05078	72.433	-.14566	24.395	.01454
				II	D	-.06778	72.442	-.14070	24.390	.01455
			.02	I	S	.15867	74.045	-.21514	21.440	.00538
				I	D	.15835	74.049	-.21454	21.435	.00536
				II	S	.02881	72.884	-.50305	23.505	.01180
				II	D	.07893	72.884	-.51482	23.486	.01165

Table 6a. (Continued)

i	$R_1=b_1^i y+b_3^i y^3$		N/S	Method	Precision	$\hat{R}_i = \hat{b}_0^i + \hat{b}_1^i y + \hat{b}_2^i y + \hat{b}_3^i y^3$				E_i
	b_1^i	b_3^i				$\hat{b}_0^i$	$\hat{b}_1^i$	$\hat{b}_2^i$	$\hat{b}_3^i$	
3	100	25	.001	I	S	-.01427	98.843	-.02418	29.512	.00446
				I	D	-.01415	98.844	-.02463	29.513	.00446
				II	S	-.07047	97.476	.38302	38.651	.01348
				II	D	-.07339	97.477	.38424	38.656	.01349
			.01	I	S	.06645	98.444	.67074	31.224	.00772
				I	D	.06663	98.444	.66983	31.226	.00772
				II	S	.03765	97.113	1.37590	41.166	.01813
				II	D	.00564	97.110	1.38350	41.184	.01787
			.02	I	S	.14580	97.925	1.34600	33.115	.01254
				I	D	.14605	97.925	1.34460	33.120	.01254
				II	S	.10024	96.607	2.38390	43.847	.02338
				II	D	.19245	96.610	2.36250	43.848	.02465
4	50	-10	.001	I	S	-.03061	49.290	.07580	-9.513	.00789
				I	D	-.03054	49.289	.07600	-9.512	.00789
				II	S	-.05281	48.922	.23406	-9.002	.01204
				II	D	-.05532	48.922	.23419	-9.002	.01203
			.01	I	S	-.05748	49.405	.05694	-9.579	.00656
				I	D	-.05664	49.404	.05627	-9.578	.00657
				II	S	-.03826	49.084	.36383	-9.207	.01192
				II	D	-.09496	49.083	.36194	-9.205	.01125
			.02	I	S	-.08937	49.501	.04032	-9.638	.00586
				I	D	-.08861	49.500	.03962	-9.638	.00586
				II	S	-.07520	49.197	.49163	-9.367	.01292
				II	D	.10552	49.199	.49369	-9.368	.01675

* I = Method I S = Single precision computations
  II = Method II D = Double precision computations

Table 6b. The coefficients of the identified damping of the second nonlinear system done by Method I and Method II in single precision and double precision calculation*.

i	$D_1=d_1^i y+d_3^i y^3$		N/S	Method	Precision	$\hat{D}_i = \hat{d}_0^i + \hat{d}_1^i y + \hat{d}_2^i y + \hat{d}_3^i y^3$				η_i
	d_1^i	d_3^i				$\hat{d}_0^i$	$\hat{d}_1^i$	$\hat{d}_2^i$	$\hat{d}_3^i$	
1	.3	.02	.001	I	S	-.00474	.36882	.00129	.01888	.04277
				I	D	-.00401	.37062	.00124	.01881	.04320
				II	S	-.00474	.36882	.00129	.01888	.04277
				II	D	-.00401	.37062	.00124	.01881	.04320
			.01	I	S	-.05902	.35145	.00412	.02035	.06029
				I	D	-.07636	.34857	.00502	.02048	.06097
				II	S	-.05902	.35144	.00412	.02035	.06029
				II	D	-.07636	.34857	.00516	.02048	.06096
			.02	I	S	-.08631	.33128	.00487	.02197	.08588
				I	D	-.03342	.34376	.00209	.02147	.08450
				II	S	-.08632	.33128	.00487	.02197	.08588
				II	D	-.03342	.34376	.00209	.02147	.08450
2	75	20	.001	I	S	.04107	.22486	-.00077	.02030	.03131
				I	D	.03890	.22599	-.00073	.02029	.03146
				II	S	.07877	.21373	-.00164	.02056	.03450
				II	D	.07516	.21539	-.00157	.02053	.03448
			.01	I	S	.10625	.23498	-.00293	.02029	.03932
				I	D	.10578	.23600	-.00292	.02028	.03947
				II	S	.15046	.23262	-.00465	.02052	.04806
				II	D	.13476	.23579	-.00444	.02048	.04838
			.02	I	S	.14124	.26213	-.00435	.02001	.04924
				I	D	.13950	.26321	-.00431	.02000	.04940
				II	S	.15053	.27719	-.00612	.02004	.06303
				II	D	.19283	.27513	-.00666	.02005	.06244

Table 6b. (continued)

i	$D_1=d_1^i y+d_3^i y^3$		N/S	Method	Precision	$\hat{D}_i = \hat{d}_0^i + \hat{d}_1^i y + \hat{d}_2^i y + \hat{d}_3^i y^3$				η_i
	d_1^i	d_3^i				$\hat{d}_0^i$	$\hat{d}_1^i$	$\hat{d}_2^i$	$\hat{d}_3^i$	
3	.2	.02	.001	I	S	.04592	.22146	-.00128	.02003	.03488
				I	D	.04708	.22193	-.00131	.02024	.03505
				II	S	.08132	.26880	-.00567	.01952	.06527
				II	D	.08153	.26875	-.00566	.01953	.06539
			.01	I	S	-.12147	.16867	.00199	.02174	.04661
				I	D	-.11962	.16906	.00193	.02173	.04644
				II	S	.05635	.24278	-.00510	.02032	.06278
				II	D	.02908	.24147	-.00493	.02034	.06287
			.02	I	S	-.02790	.13032	.00516	.02279	.07451
				I	D	-.27858	.13092	.00515	.02278	.07438
				II	S	.00825	.22404	-.00259	.02094	.06332
				II	D	.10102	.22733	-.00345	.02091	.06714
4	.1	.02	.001	I	S	-.13261	.22245	.00044	.01800	.04685
				I	D	-.11423	.22502	-.00023	.01790	.04670
				II	S	-.09444	.20412	.00459	.01831	.04304
				II	D	-.07378	.20734	.00374	.01822	.04266
			.01	I	S	-.24066	.22469	.00251	.01820	.05645
				I	D	-.22695	.22739	.00199	.01813	.05628
				II	S	-.00806	.19753	.00824	.01835	.05739
				II	D	-.04552	.20146	.00749	.01825	.05326
			.02	I	S	-.28979	.23868	.00268	.01811	.06659
				I	D	-.28567	.23928	.00225	.01809	.06649
				II	S	.03103	.20477	.01147	.01809	.07794
				II	D	.21830	.20312	.01119	.01810	.09804

*I = Method I

II = Method II

S = single precision computations

D = double precision computations

Table 7. Comparison of the identified coefficients of the second nonlinear system in separable restoring force case by the separable restoring force(s) and the general restoring force (G) in Method I and single precision calculation.

i	$K=b_1^i y+b_3^i y^3+d_1^i \dot{y}+d_3^i \dot{y}^3$				N/S	R.F.	$K[y_\ell, \dot{y}_\ell] = a_0^i + a_1^i y + a_2^i y^2 + a_3^i y^3 + a_4^i \dot{y}_\ell + a_5^i \dot{y}_\ell + a_6^i \dot{y}_\ell^3$							η_i
	b_1^i	b_3^i	d_1^i	d_3^i			a_0^i	a_1^i	a_2^i	a_3^i	a_4^i	a_5^i	a_6^i	
						S	.02160	48.375	-.04160	12.375	.36882	.00129	.01888	.04510
					.001	G	.00021	49.997	-.00728	9.970	.29566	-.00014	.02067	.00024
1	50	10	.3	.02		S	.10546	48.628	-.02344	11.606	.35145	.00412	.02035	.06152
					.01	G	.01535	49.937	-.99801	7.543	.37732	-.00208	-.0043	.05756
						S	.15850	48.700	-.03590	11.109	.33128	.00487	.02197	.08700
					.02	G	.07649	50.552	-5.9160	-4.168	.44665	-.02794	-.02717	.11509
						S	.00115	73.254	.10587	22.916	.22486	-.00077	.02030	.03275
					.001	G	.00098	74.999	-.15306	20.054	.19541	-.00064	.02026	.00011
2	75	20	.2	.02		S	.16591	73.669	-.06598	22.185	.23498	-.00292	.02029	.04000
					.01	G	.01562	74.562	-.29300	21.541	.21931	-.00395	.01926	.03259
						S	.29991	74.045	-.21514	21.440	.26213	-.00435	.02001	.04953
					.02	G	.02943	73.992	-.42824	22.887	.24299	-.00703	.01801	.06518
						S	.03165	98.843	-.02418	29.512	.22146	-.00128	.02025	.03517
					.001	G	.00035	100.01	.04555	24.785	.19621	-.00036	.02087	.00005
3	100	25	.2	.02		S	.05502	98.444	.67074	31.224	.16867	.00199	.02174	.04725
					.01	G	-.10294	99.706	.96673	24.804	.29445	.01986	.01823	.03422
						S	.13320	97.925	1.34600	33.115	.13030	.00516	.02279	.07556
					.02	G	-.19759	99.228	1.89125	24.704	.37880	.03640	.01822	.06835
						S	.16322	49.290	.07579	-9.512	.22245	.00044	.01797	.04750
					.001	G	-.00004	49.999	.00324	-10.00	.09502	-.00044	.02033	.00047
4	50	-10	.1	.02		S	-.29814	49.405	.05694	-9.579	.22469	.00251	.01820	.05683
					.01	G	.01860	50.085	.16231	-10.352	-.00928	-.03925	.01660	.03874
						S	.37916	49.501	.04032	-9.638	.23868	.00240	.01811	.06685
					.02	G	.03456	50.156	.33714	-10.732	-.10973	-.07193	.11261	.07734

Table 8. The exact parameters and the identified corresponding terms used in the general restoring force case.

ℓ	N/S	$K_\ell[y_\ell,\dot{y}_\ell] = a^1_\ell y_\ell + b_\ell y^3_\ell + c_\ell y_\ell \dot{y}^2_\ell + d_\ell \dot{y}_\ell + e_\ell \dot{y}^2_\ell + f_\ell \dot{y}_\ell y^2_\ell$						η
		a_ℓ	b_ℓ	c_ℓ	d_ℓ	e_ℓ	f_ℓ	
	EXACT	50.	10.	10.	.3	.02	0.0	
	.001	49.961	9.743	10.010	.29432	.01974	.105	.00423
1	.01	50.083	1.067	10.014	.17897	.01090	15.467	.04473
	.02	48.998	5.400	9.9320	.00280	.01350	33.825	.09205
	EXACT	75.	20.	0.0	.2	.02	.2	
	.001	75.156	17.030	-.0617	.1925	.0211	2.8926	.00116
2	.01	75.493	17.097	-.0819	.2172	.0168	1.6016	.01180
	.02	74.262	49.431	-.1786	.2426	.01302	.7544	.03081
	EXACT	100	25	10.0	.2	.02	0.0	
	.001	99.946	21.343	9.9850	.32668	.00575	-17.90	.00094
3	.01	97.829	44.649	10.671	.37731	.01309	3.53	.01066
	.02	88.006	25.434	-2.2157	.47349	.01451	11.718	.02708
	EXACT	50	-10	0.0	.1	.02	.2	
	.001	49.949	-9.990	.03473	.08053	.02963	.19440	.00136
4	.01	49.484	-9.870	.35721	-.06194	.10968	.13410	.01341
	.02	48.997	-9.879	.6953	-.21806	.19722	.07924	.02677

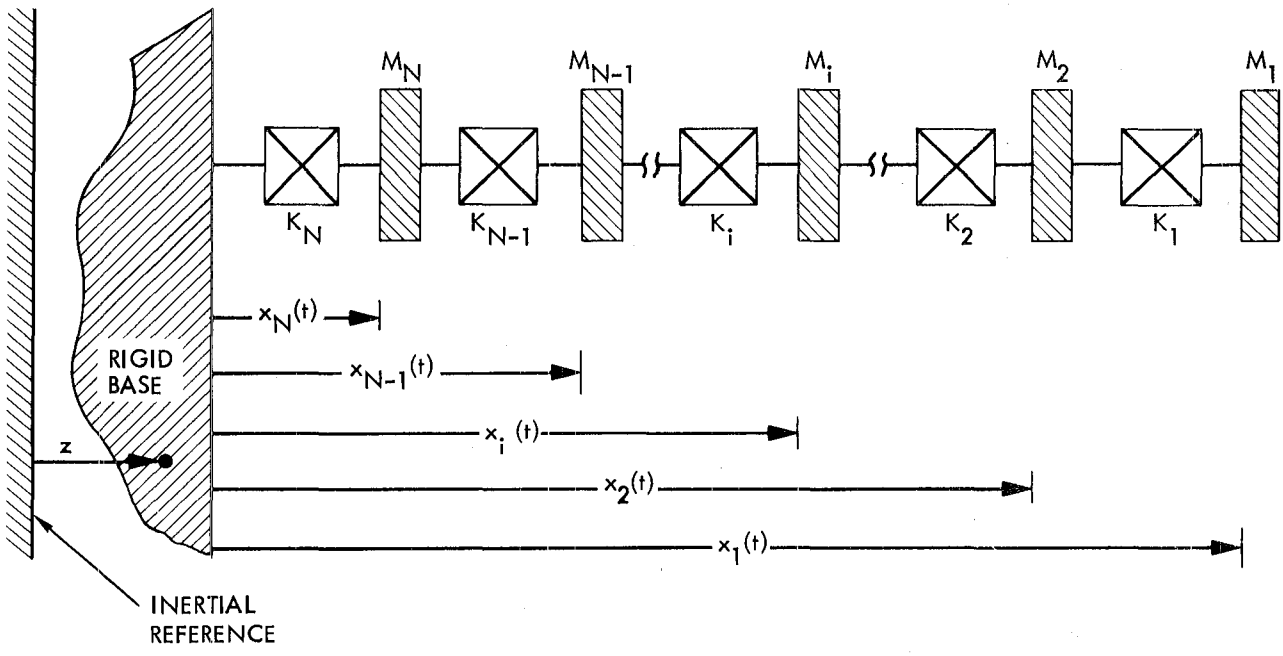

Figure 1. Close-coupled system

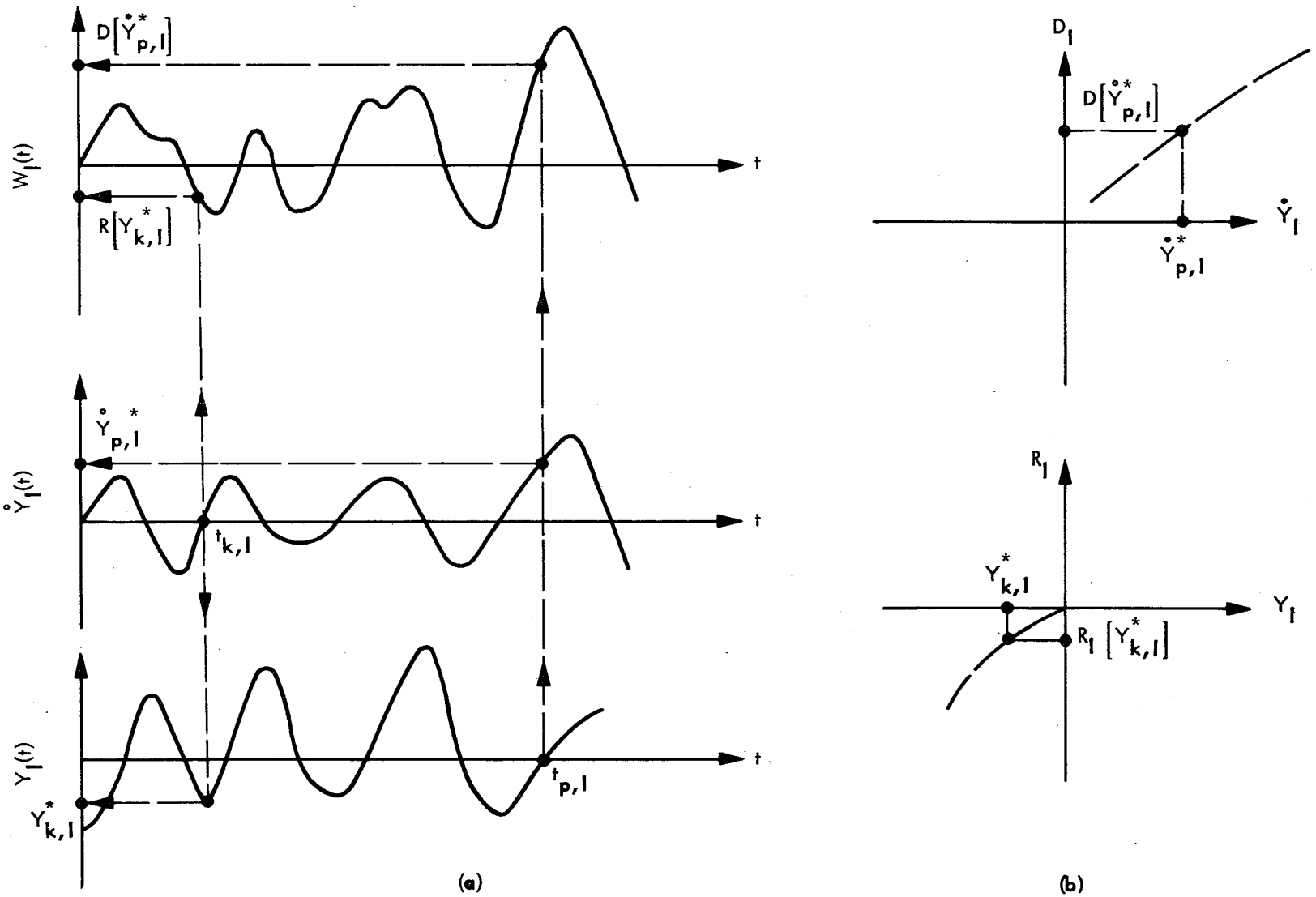

Figure 2. Interpolation of zero velocity (landscape)

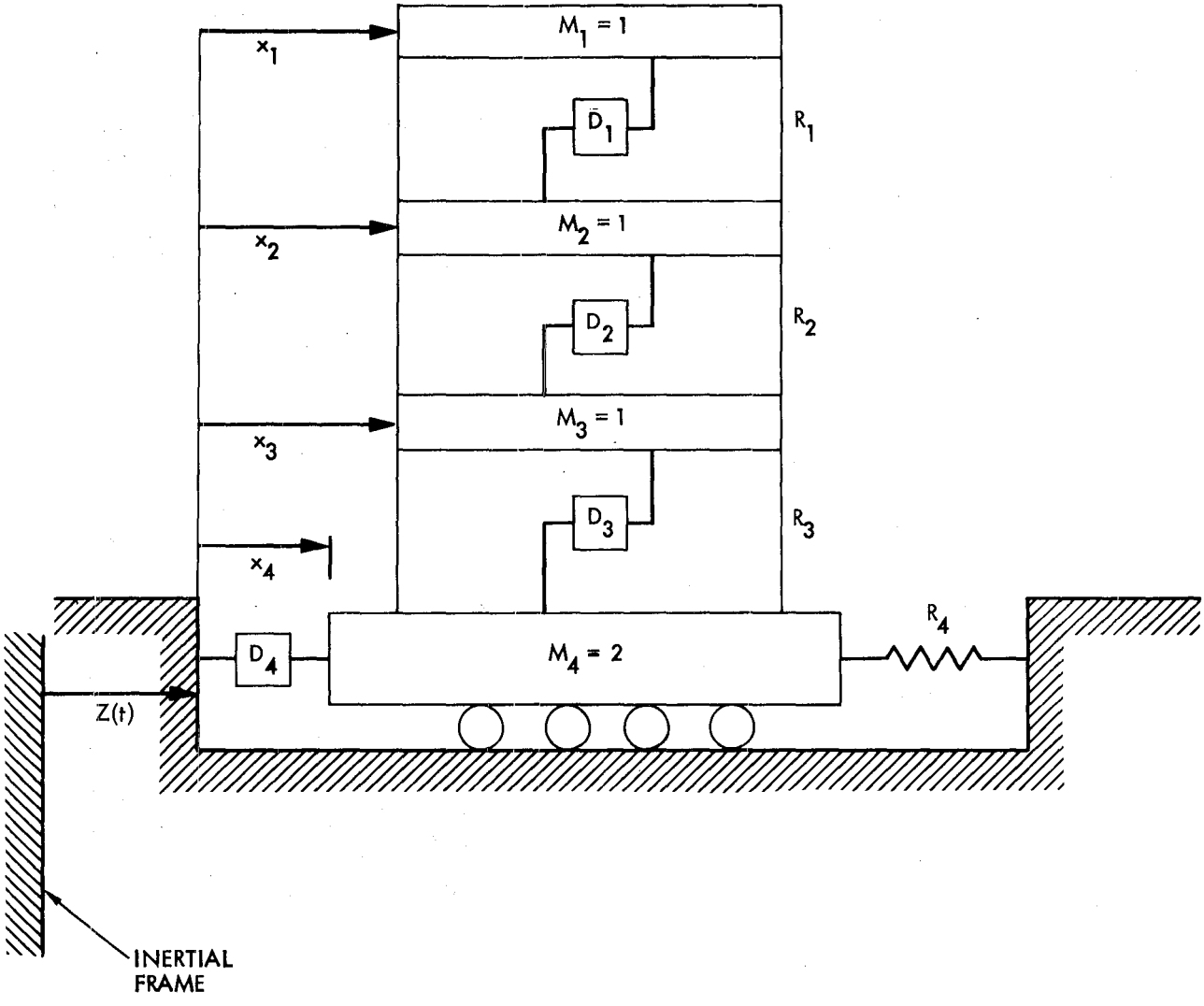

Figure 3. Four-degree-of-freedom example

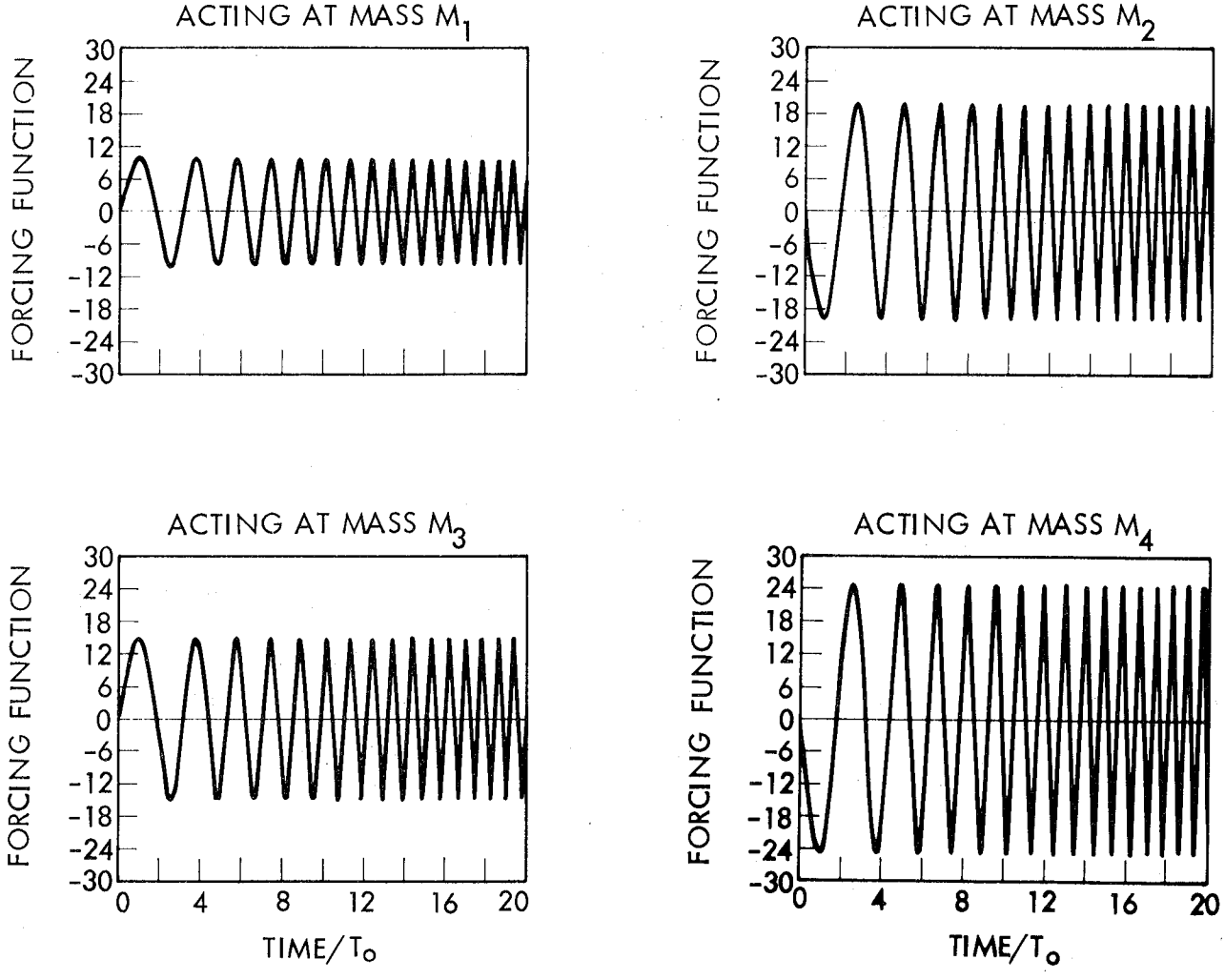

Figure 4. Swept-sine test signal for identification.

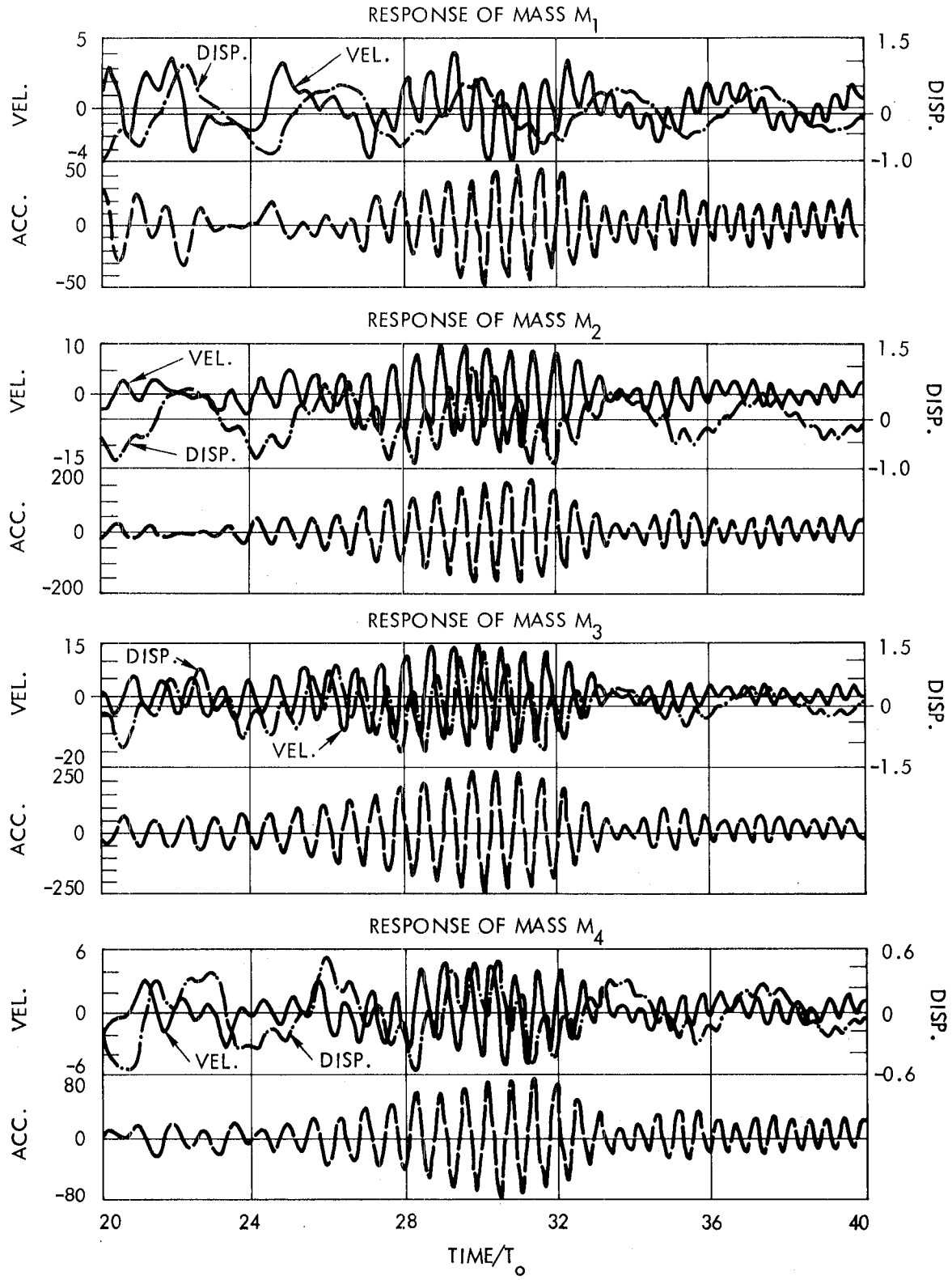

Figure 5. Response of linear system to swept sine forcing.

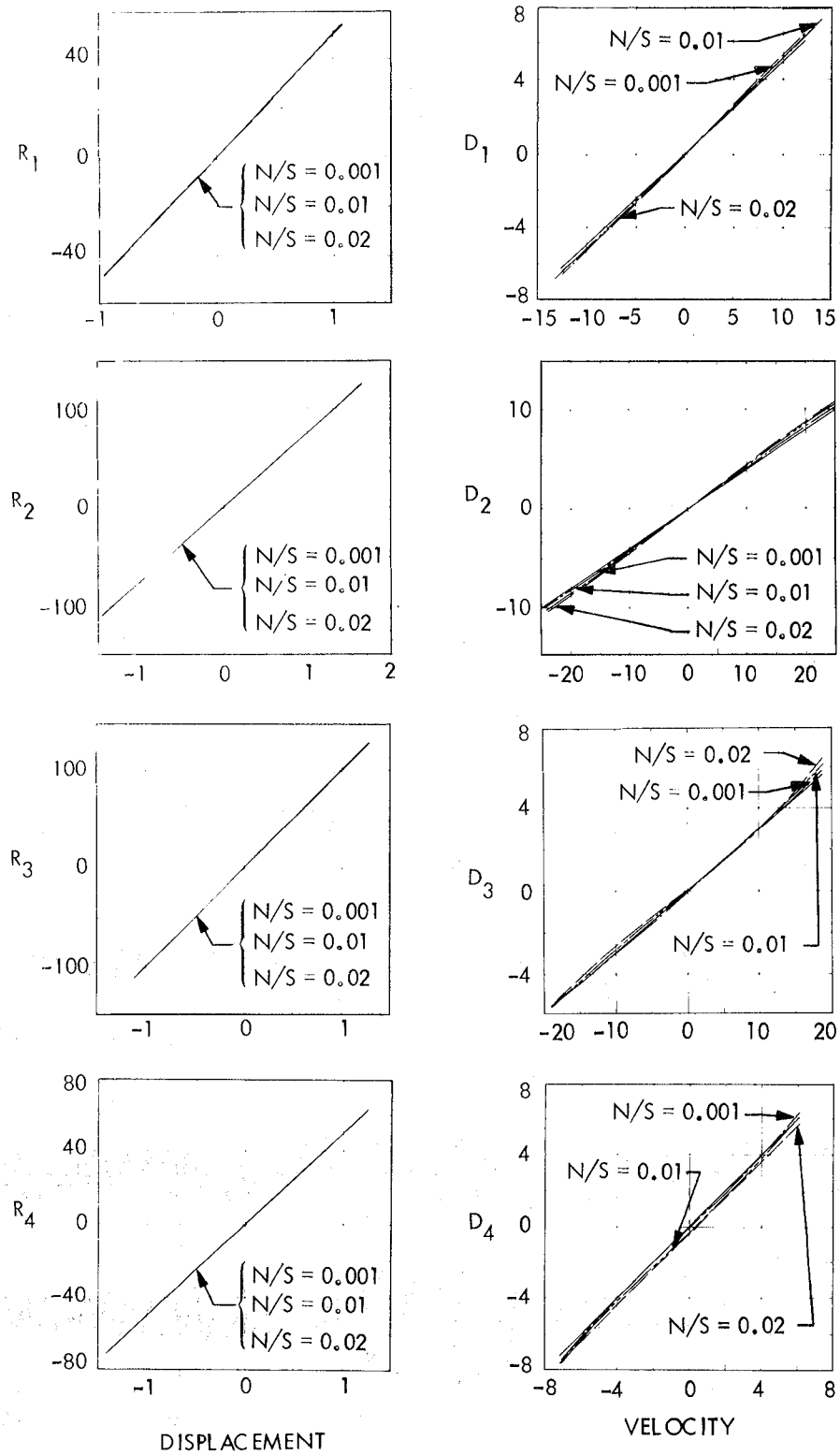

Figure 6. A comparison of the actual stiffness and damping denoted by solid (—) lines and the identification results with 0.1% noise (— - —), with 1% noise (— - - —), and with 2% noise (— — —) for System 1.

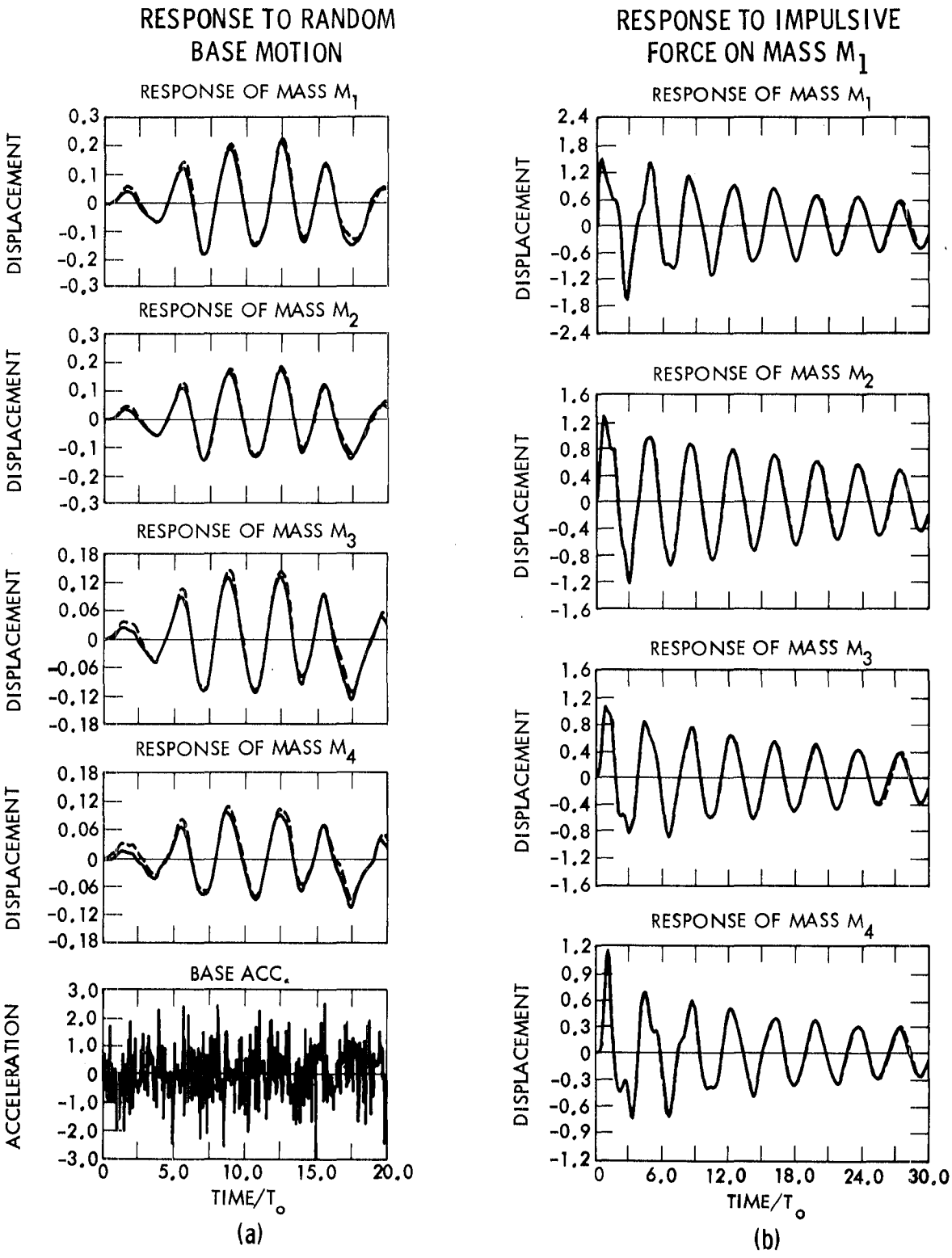

Figure 7. A comparison of the response of the actual system (—) with that of the identified system (— — —), (a) under base excitation, (b) under an impulse force of the ten units applied at M_1 for System 1.

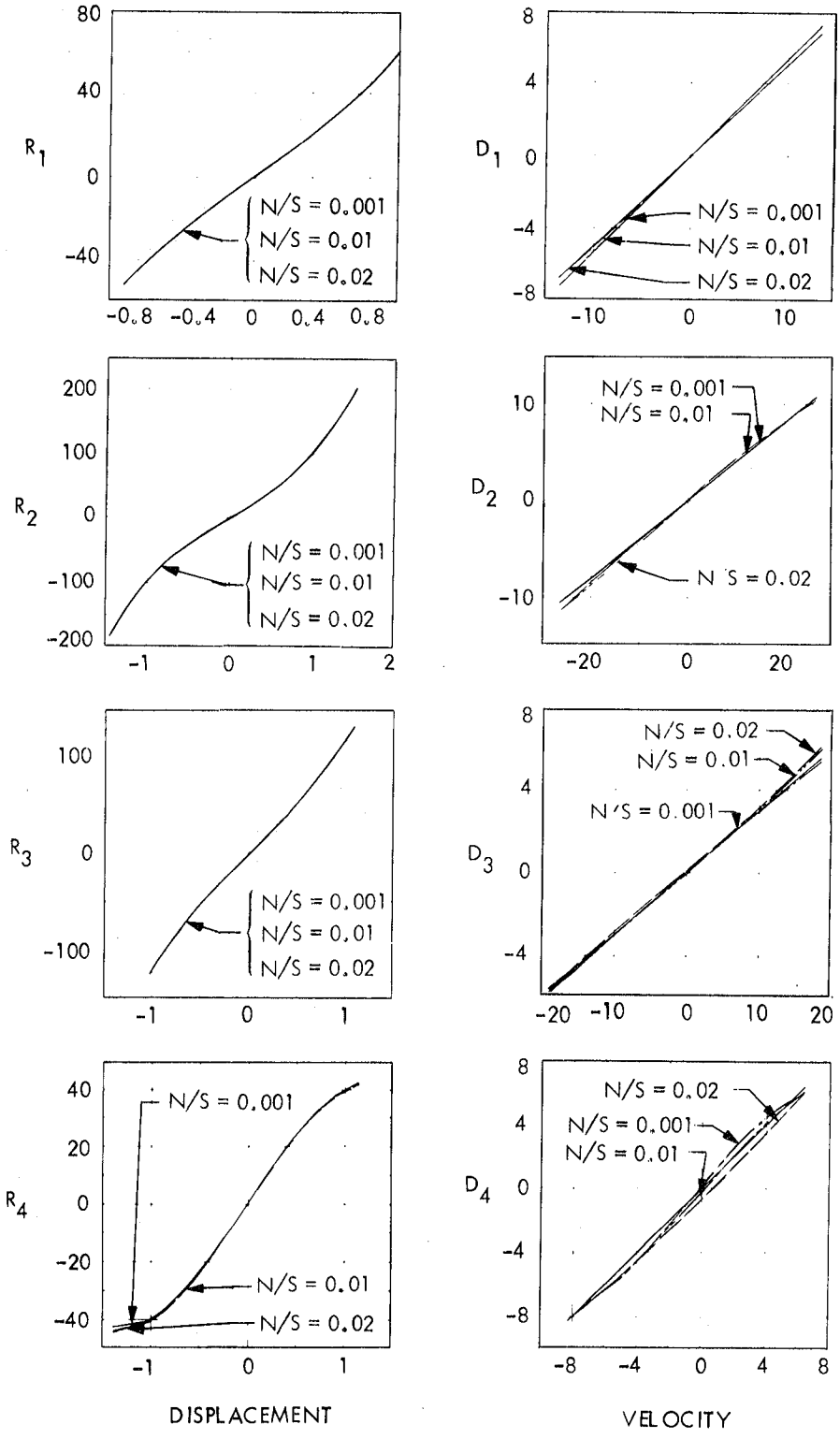

Figure 8. A comparison of the actual stiffness and damping denoted by solid (—) lines and the identification results with 0.1% noise (— - —), with 1% noise (— - - —), and with 2% noise (— — —) for System 2.

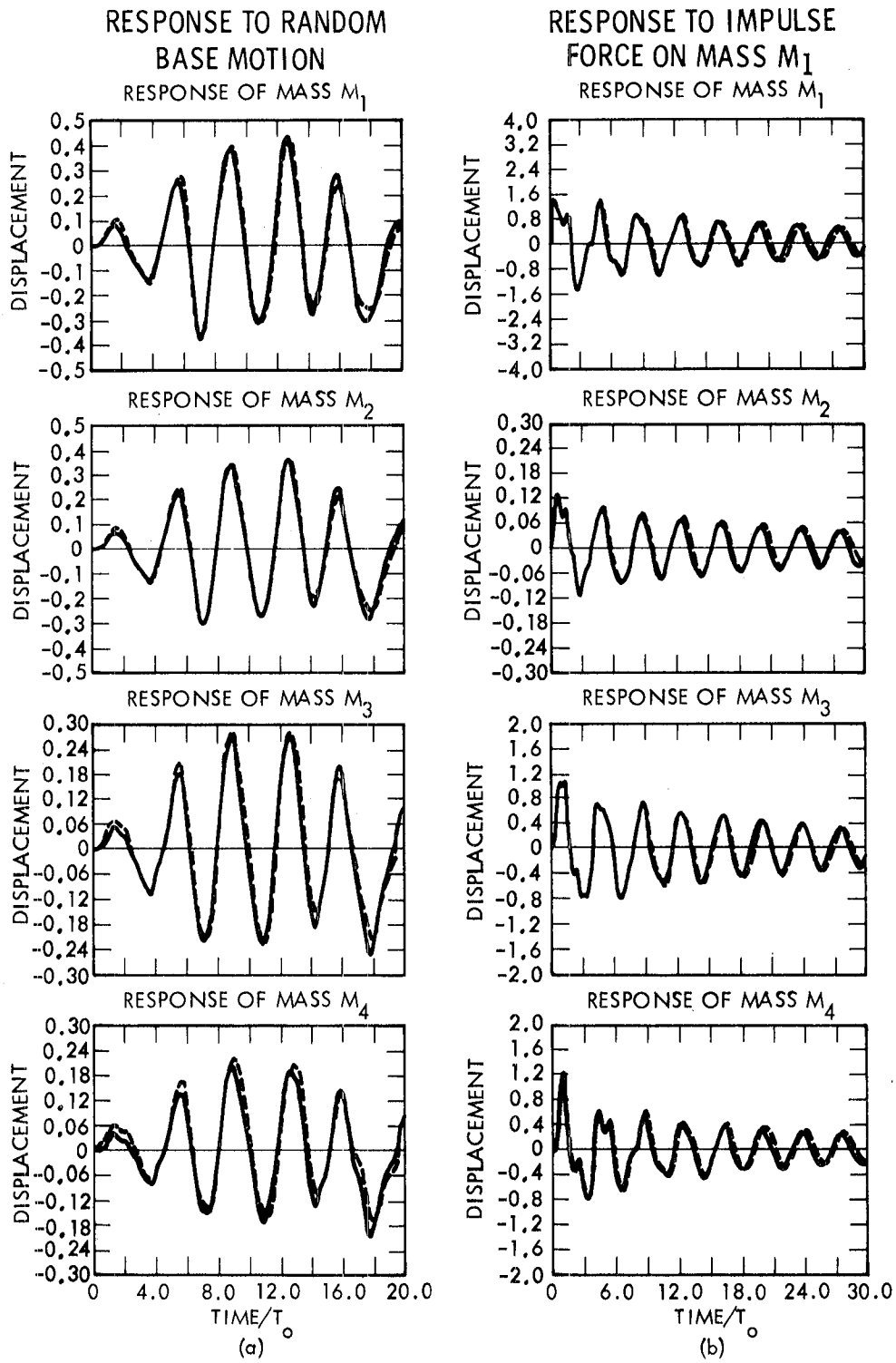

Figure 9. A comparison of the response of the actual system (—) with that of the identified system (— — —), (a) under base excitation, (b) under an impulse force of the ten units applied at M_1 for System 2.

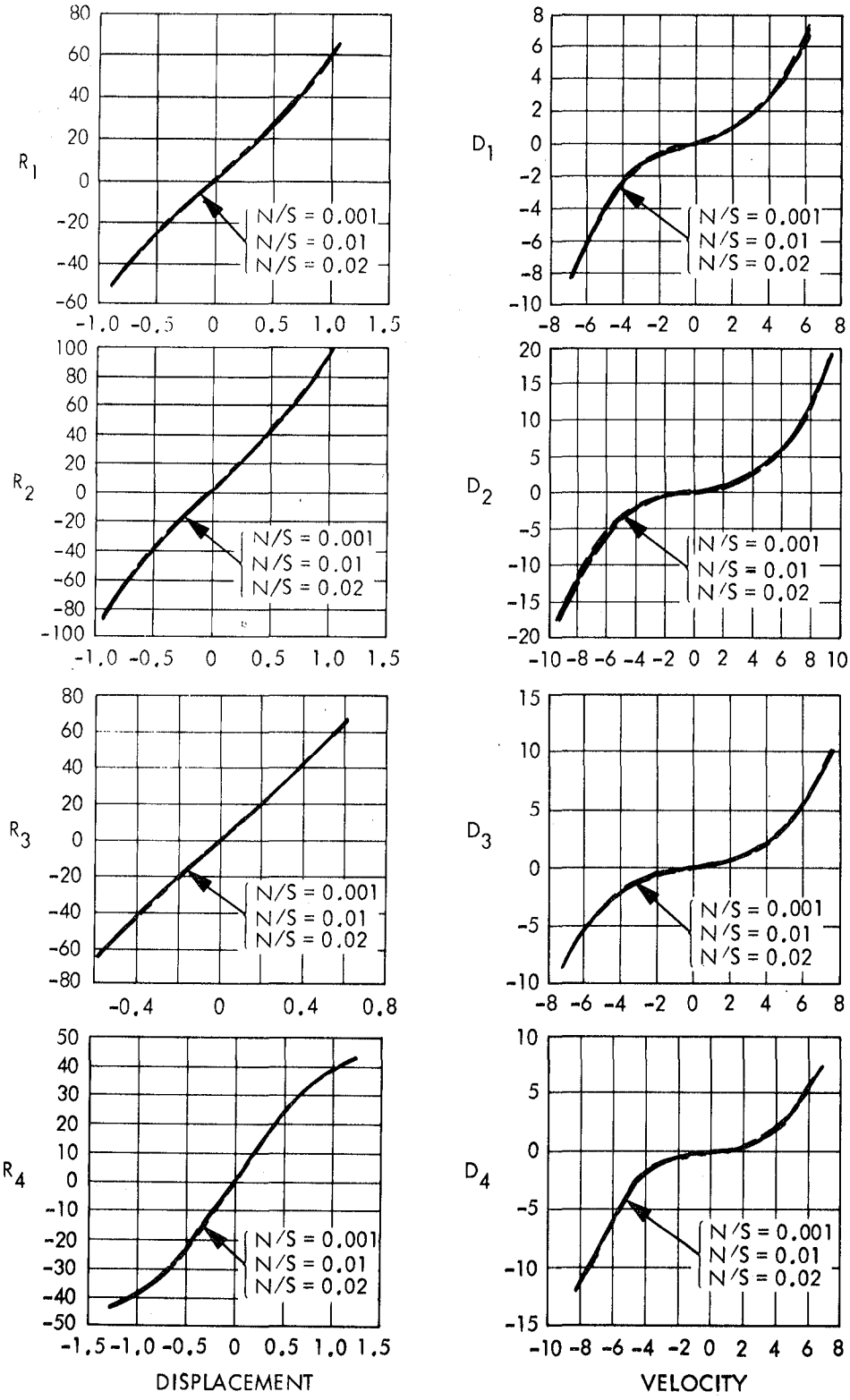

Figure 10. A comparison of the actual stiffness and damping denoted by solid (—) lines and the identification results with 0.1% noise (— - —), with 1% noise (— - - —), and with 2 % noise (— — —) for System 3.

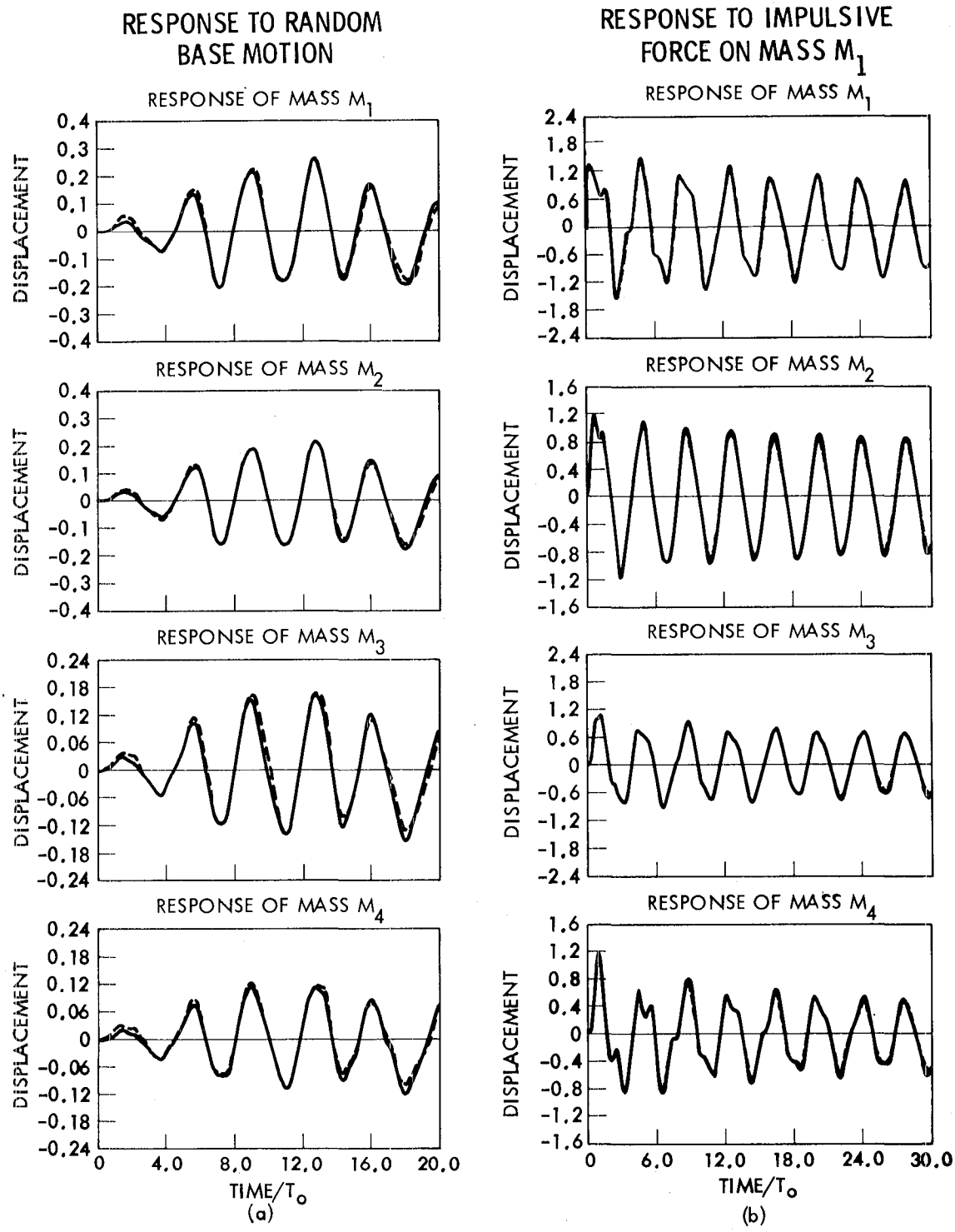

Figure 11. A comparison of the response of the actual system (—) with that of the identified system (— — —), (a) under base excitation, (b) under an impulse force of the ten units applied at M_1 for System 3.

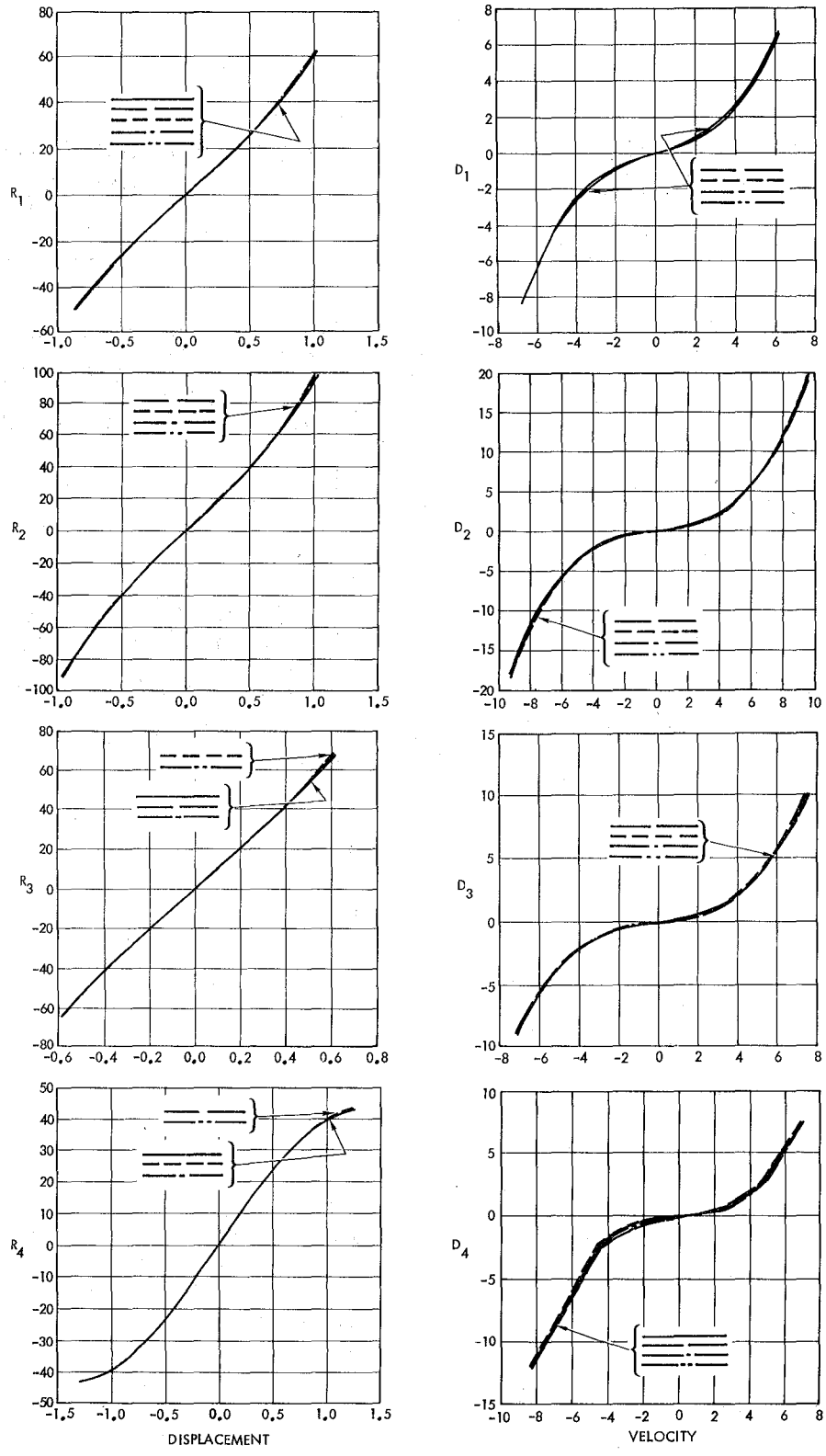

Figure 12. A comparison of actual stiffness and damping denoted by solid (—) lines and the identified results by Method I and single precision (— —), Method I and double precision (----), Method II and single precision (— - —) and Method II and double precision (— - - —) in nonlinear case (1-b) of N/S = 0.001.

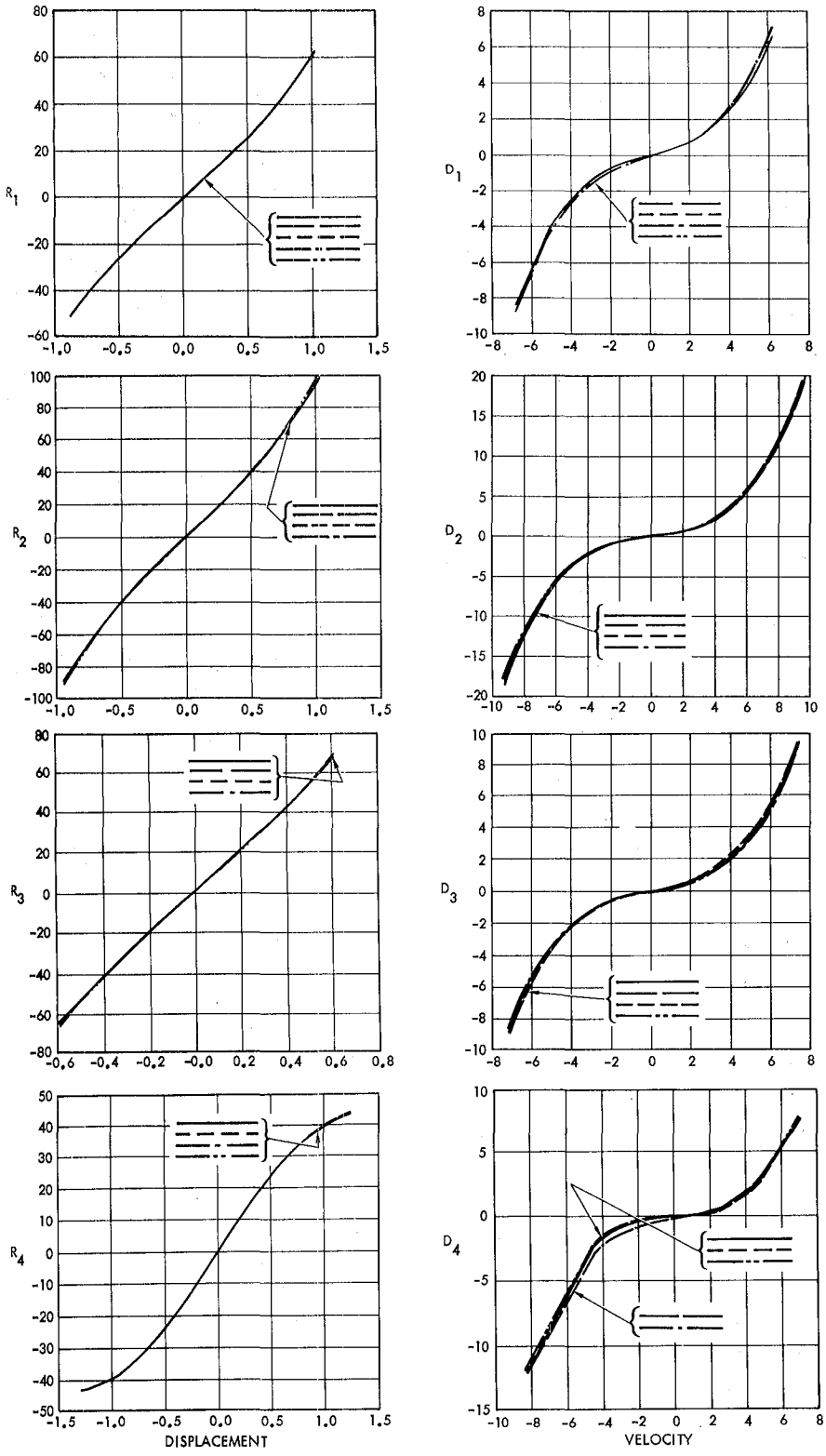

Figure 13. A comparison of actual stiffness and damping denoted by solid (—) lines and the identified results by Method I and single precision (— —), Method I and double precision (----), Method II and single precision (— - —) and Method II and double precision (— - - —) in nonlinear case (1-b) of N/S = 0.01.

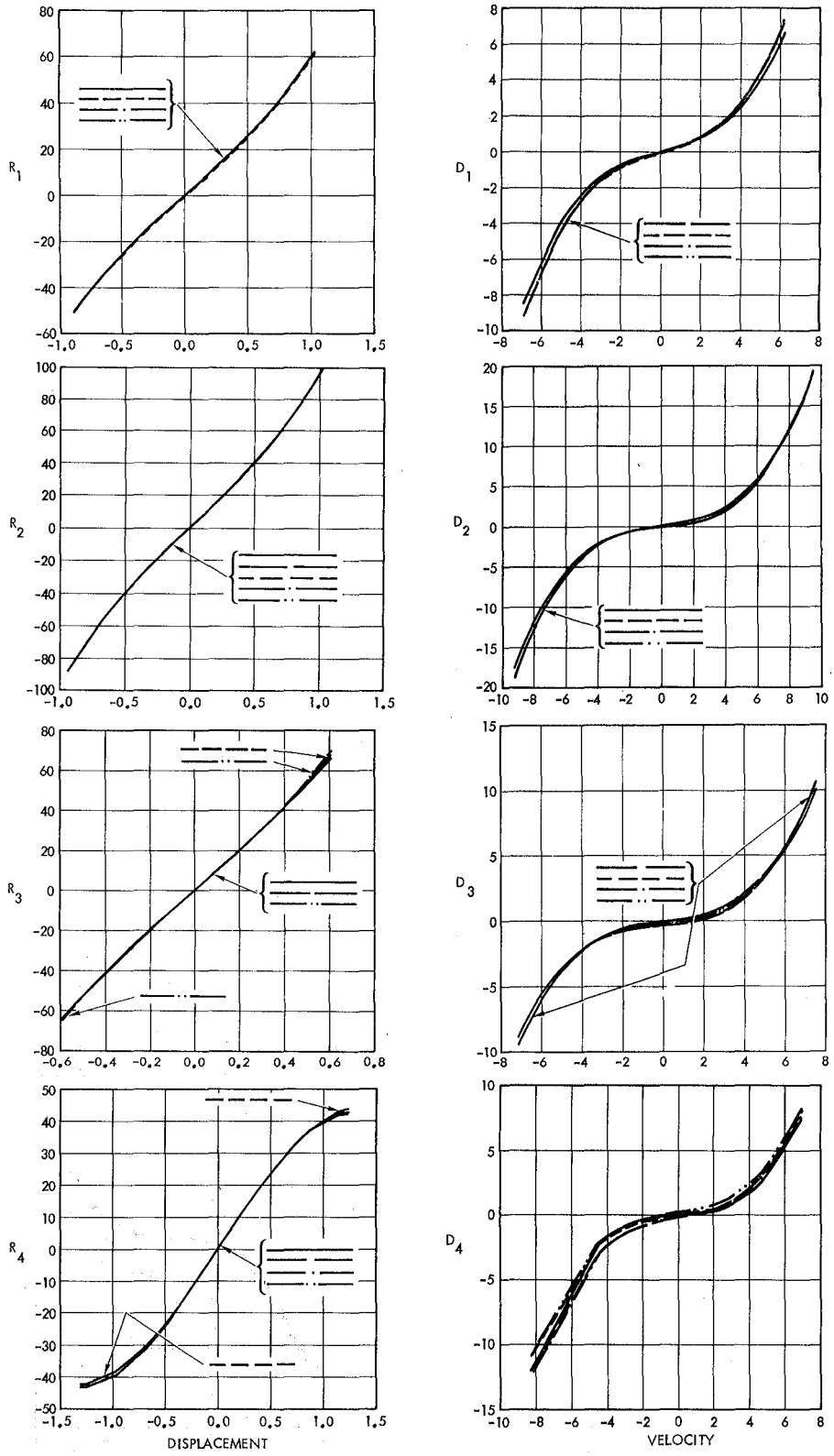

Figure 14. A comparison of actual stiffness and damping denoted by solid (—) lines and the identified results by Method I and single precision (— —), Method I and double precision (----), Method II and single precision (— - —) and Method II and double precision (— - - —) in nonlinear case (1-b) of N/S = 0.02.

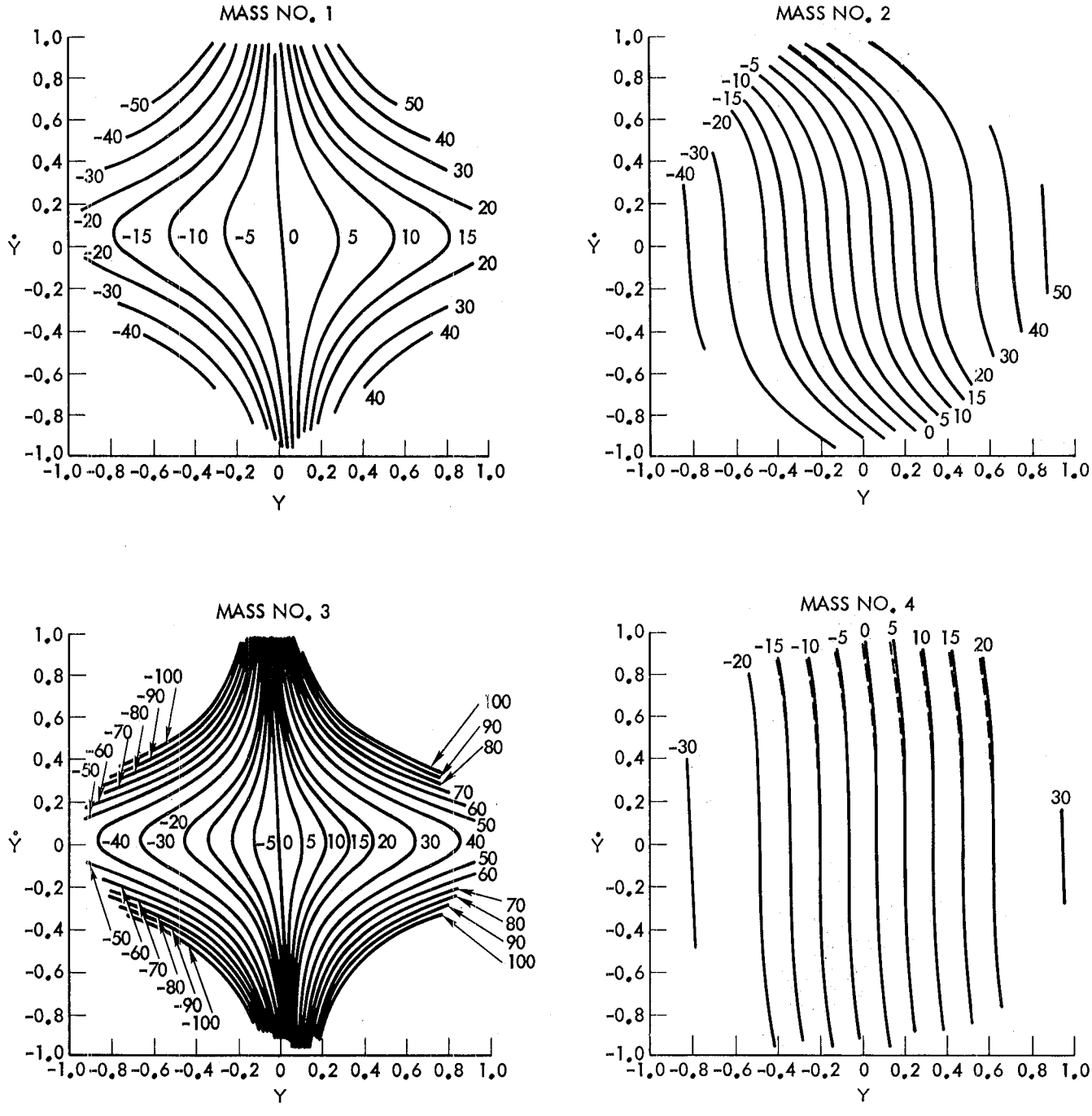

Figure 15. A comparison of actual restoring force denoted by solid (—) line and the results identified by the general restoring force method (----) for the general restoring force case with N/S = 0.001.

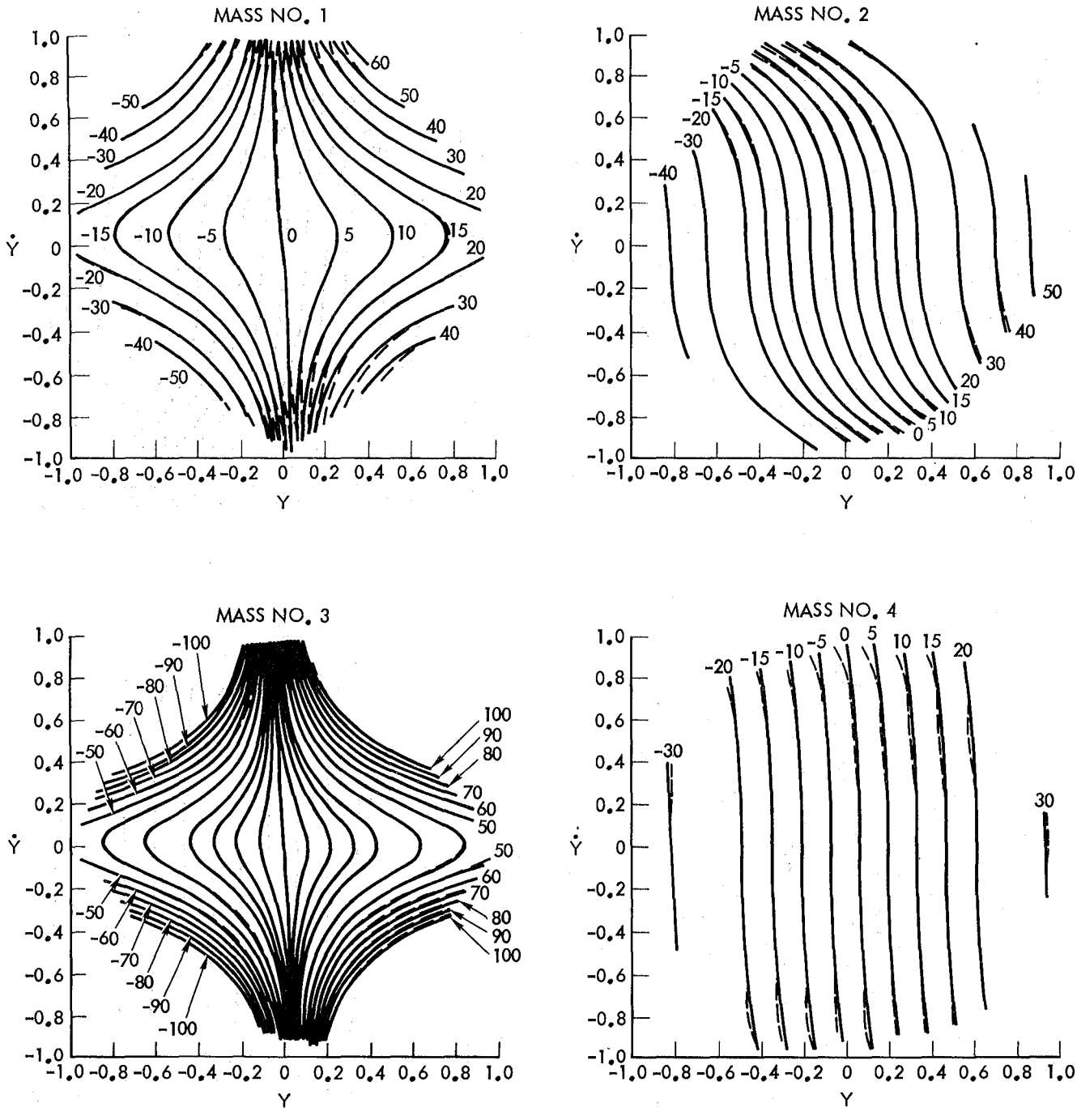

Figure 16. A comparison of actual restoring force denoted by solid (—) line and the results identified by the general restoring force method (----) for the general restoring force case with N/S = 0.01.

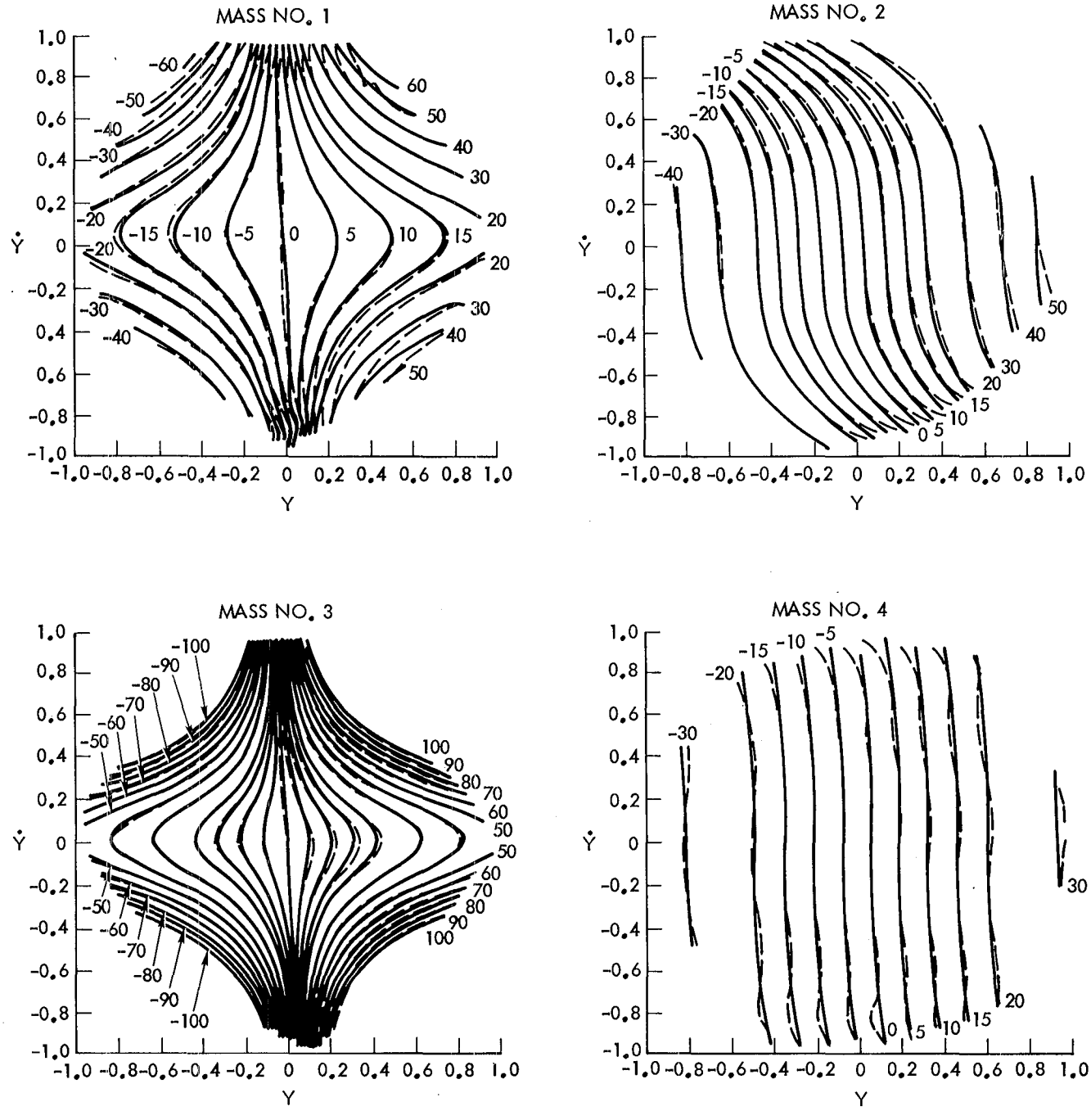

Figure 17. A comparison of actual restoring force denoted by solid (—) line and the results identified by general restoring force method (----) for the general restoring force case with N/S = 0.02.

End of Document